Nanoscale Advances

ROYAL SOCIETY OF CHEMISTRY

REVIEW

View Article Online
View Journal | View Issue



Cite this: *Nanoscale Adv.*, 2025, **7**, 1226

# Emerging engineered nanozymes: current status and future perspectives in cancer treatments

Jiajia Zheng,†[ab] Weili Peng,†[b] Houhui Shi,[bc] Jiaqi Zhang,[b] Qinglian Hu [a] and Jun Chen *[b]

Received 8th November 2024
Accepted 10th January 2025

DOI: 10.1039/d4na00924j

rsc.li/nanoscale-advances

Composite nanozymes are composed of enzymes with similar or different catalytic capabilities and have higher catalytic activity than a single enzyme. In recent years, composite nanozymes have emerged as novel nanomaterial platforms for multiple applications in various research fields, where they are used to produce oxygen, consume glutathione, or produce toxic reactive oxygen species (ROS) for cancer therapy. The therapeutic approach using composite nanozymes is known as chemo-dynamic therapy (CDT). Some composite nanozymes also show special photothermal conversion effects, enabling them to be combined with pioneering cancer treatments, such as photodynamic therapy (PDT), photothermal therapy (PTT) and sonodynamic therapy (SDT), and enhance the anti-cancer effects. In this study, the classification and catalytic performances of composite nanozymes are reviewed, along with their advantages and synthesis methods. Furthermore, the applications of composite nanozymes in the treatment of cancers are emphasized, and the prospective challenges in the future are discussed.



## 1. Introduction

The incidence and mortality rates of cancer are rising, with close to 20 million newly diagnosed cases and 9.7 million deaths recorded in 2022.[1] This data represent a significant increase of 41.84% and 18.29%, respectively, compared to the 14.1 million cases and 8.2 million deaths reported in 2012.[2] Cancer has emerged as a grave threat to human life and well-being, ranking as the second leading cause of death worldwide.[3] Conventional therapies, such as surgery, radiotherapy (RT), and chemotherapy (CTx), exhibit notable side effects, often encounter drug resistance, and frequently fall short of achieving the desired outcomes.[4] Consequently, researchers have been exploring novel cancer treatment methods, with nanotechnology emerging as one of the most promising approaches.[5]

The specificity of tumors makes their treatment difficult. The pro-angiogenic factors secreted by tumor cells lead to the formation of an abnormal tumor vascular network, which is disorganized, immature and poorly permeable, leading to poor tumor perfusion. At the same time, owing to the rapid growth of tumor tissues, a large amount of oxygen and nutrients are getting consumed, eventually leading to hypoxia in the tumor microenvironment (TME).[6] However, in an anoxic environment, tumor cells alter the expression of glycolytic related proteins, such as GLUT1, GLUT3, LDHA, and PKM2, increasing glucose uptake to promote their growth, and an anoxic environment also induces epithelial–mesenchymal transformation, thereby increasing the production of matrix metalloproteinases (MMPs), which promote aggressive metastasis.[7]

The hypoxic tumor microenvironment not only promotes tumor growth, metastasis and the evasion of immunosuppression but also inhibits the efficacy of various oxygen-dependent therapies. For instance, the efficacy of radiotherapy is suppressed mainly because of hypoxia. In addition, most non-invasive new cancer therapies that have attracted much attention in recent years, such as PDT and SDT, are based on oxygen. Changing the anoxic microenvironment of the tumor is an effective prerequisite strategy to treat tumors.

The content of ROS in solid tumors is higher than that in normal cells (from 100 μM to 1 mM), especially for $H_2O_2$, which is the most prevalent and stable non-free radical ROS in cancer cells, and these ROS promote the occurrence and development of tumors as well as promote the metastasis of tumors.[8] On the one hand, using endogenous $H_2O_2$ to generate oxygen and change the hypoxic microenvironment of tumors can improve the treatment efficiency of various oxygen-dependent therapies, which is conducive to overcoming cancer. On the other hand, the use of $H_2O_2$ to generate other types of ROS that cause fatal damage to cancer cells, such as hydroxyl radicals (·OH), can significantly enhance the oxidative damage to tumors and induce the apoptosis of cancer cells. In addition, some

[a]College of Biotechnology and Bioengineering, Zhejiang University of Technology, Hangzhou, Zhejiang, China. E-mail: huqinglian@zjut.edu.cn

[b]Cancer Center, Department of Interventional Medicine, Zhejiang Provincial People's Hospital (Affiliated People's Hospital), Hangzhou Medical College, Hangzhou, Zhejiang, China. E-mail: chenjun@hmc.edu.cn

[c]College of Pharmaceutical Science, Zhejiang University of Technology, Hangzhou, Zhejiang, China

† These authors contributed equally to this work.

nanozymes can convert $O_2$ into superoxide anion free radicals ($\cdot O_2^-$) or $H_2O_2$, and some can convert $\cdot O_2^-$ into $H_2O_2$, so as to supplement $H_2O_2$ and improve treatment efficiency.

Since the initial discovery of ferromagnetic nanozymes ($Fe_3O_4$ NPs) exhibiting peroxidase (POD) activity in 2007,[9] nanozyme technology has been continuously developed, with many new nanozymes reported. Nanozymes are artificial enzyme that have a high enzyme-like catalytic activity and can regulate biochemical reactions. Nanozymes include several categories, such as metal-, metal oxide-, MXene-, carbon-, and metal–organic framework (MOF)-based nanozymes.[10] They have attracted significant attention due to their high operational stability, work efficiency under extreme conditions, and resistance to protease digestion. Nanozymes can effectively replace natural enzymes in catalytic reactions, as they closely resemble natural enzymes in their active sites. Table 1 summarizes the advantages and limitation of nanozymes and conventional enzymes.[11] For instance, most nanozymes can mimic the activities of oxidoreductases, such as POD,[12] oxidase (OXD), catalase (CAT),[13] and superoxide dismutase (SOD).[14] Additionally, the nanomaterial characteristics of nanozymes provide them with enhanced stability surpassing that of natural enzymes. Moreover, their unique nanoscale dimensions facilitate efficient distribution within organisms and enable their accumulation at tumor sites through an enhanced permeability and retention (EPR) effect.[15] Fig. 1 and Table 2 summarize the types of nanozymes and their principle functions and characteristics in cancer therapy.

Nanozymes of a specific class may exhibit a spectrum of catalytic activities; for instance, copper nanoparticles (Cu NPs) typically possess POD and OXD activities. However, under specific conditions, such as variations in pH, particle size and morphology, or ion valence states, these nanozymes often manifest a single catalytic capability. To emulate the concatenated enzymatic reactions observed in natural systems, the development of composite nanozymes has been pursued as a feasible strategy.[43] For instance, Hao *et al.* synthesized clusters of copper oxide nanoparticles ($Cu_xO$ NPs), comprising a mixture of CuO and $Cu_2O$, and demonstrated that these composite nanozymes could serve as antioxidants by functioning concurrently as CAT, GPx, and SOD analogs.[44] Similarly, Ling *et al.* fabricated copper@copper(I) oxide aerogel networks ($Cu@Cu_2O$) and identified their dual enzymatic mimicry, exhibiting activities analogous to both horseradish peroxidase (HRP) and NADH peroxidase.[45] It is thus evident that the amalgamation of two or more nanozymes with analogous functionalities can result in an enhanced catalytic potency compared to the individual constituents of the nanozymes alone. For instance, Boruah *et al.* synthesized a composite nanozyme comprising $Fe_3O_4$, $TiO_2$, and reduced graphene oxide (rGO), and observed that the POD activity of the resulting composite enzyme was significantly more robust than the intrinsic POD activities of the individual components, namely $Fe_3O_4$ NPs, $TiO_2$ NPs, and rGO.[46]

There are many reviews that have extensively covered the topic of nanozymes;[14,15,47] however, there is a lack of literature specifically summarizing the application of composite nanozymes in cancer treatment. Consequently, in this article we review the catalytic activity and therapeutic mechanisms of common nanozymes in cancer treatment. We also examine the classification and benefits of composite nanozymes, present various synthesis methods for these composite nanozymes, and describe their applications in combination with different therapeutic approaches for various cancers. The discussion concludes with an exploration of the remaining challenges and future directions for composite nanozymes.

## 2. Introduction to composite nanozymes

In order to improve the catalytic efficiency of nanozymes and optimize therapeutic outcomes, composite nanozymes have been proposed. These composite nanozymes can incorporate a combination of nanozymes with the same or different catalytic functions, including inorganic enzymes and organic enzymes, and artificial enzymes and natural enzymes. In addition to augmenting specific catalytic abilities or enabling multifunctional catalysis, some enzymes are also endowed with other properties after being made into composite nanozymes, such as magnetism, or photothermal properties, that were not originally available. Fig. 2 summarizes the composition and application of composite nanozymes in different fields and their various advantages.

### 2.1 Classification of composite nanozymes

Composite nanozymes can be categorized into artificial enzymes and artificial–natural enzyme complexes in terms of

Table 1 Comparison between nanozymes and conventional enzymes

| | Nanozymes | Enzymes |
|---|---|---|
| Advantages | High stability, resistant to protease digestion | Highly selective about the targets |
| | Enters the tumor through an EPR effect | Mild conditions |
| | Large specific surface area for surface modification and bioconjugation | Environmentally friendly |
| | Simple synthesis method, low cost | |
| | High stable biocatalytic activity | |
| Limitations | Low specificity, accelerate the production of harmful free radicals in normal tissues | High cost |
| | | Low yield and storage challenges |
| | Limited species of catalytic activity | Poor stability |
| | Toxicity in some nanozymes | Substrate restriction |
| | Low activity | Catalytic activity is easily inhibited |

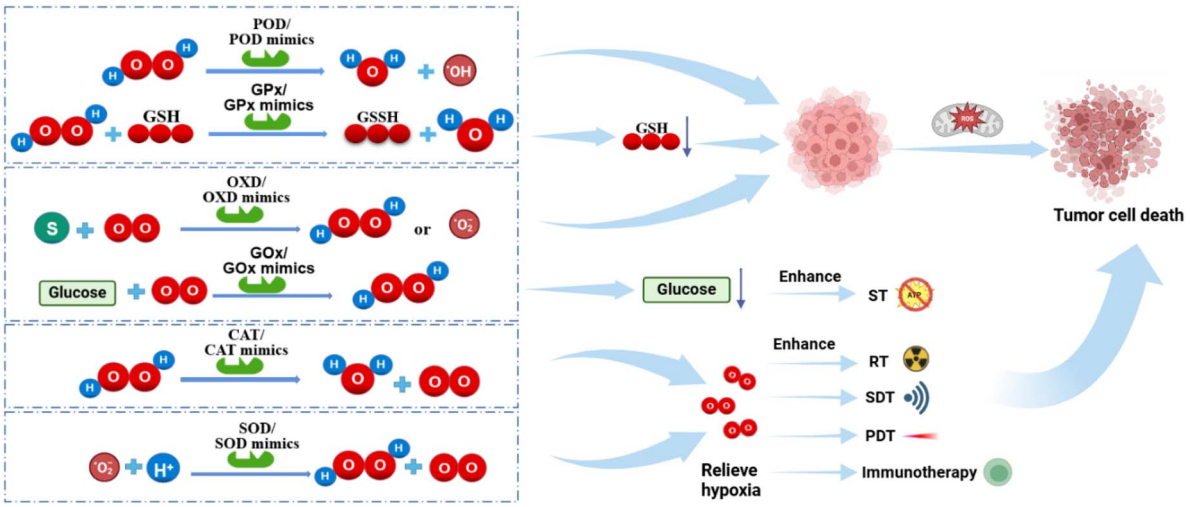


Fig. 1 Schematic indicating the different catalytic activities of common nanozymes, including POD enzyme and a typical POD enzyme (glutathione peroxidase, GPx), OXD enzyme and a typical OXD enzyme (glucose oxidase, GOx), CAT enzyme and SOD enzyme. It introduces the principles of action of these nanozymes with diverse activities in tumor therapy, including the induction of apoptosis through ROS generation and adjustment of the TME to collaborate with other therapeutic strategies in facilitating cell demise.

Table 2 Nanozymes and their application in cancer therapy

| Type | Catalytic reaction | Example | Application in cancer therapy |
|---|---|---|---|
| POD | Catalyze $H_2O_2$ into $H_2O$ and ·OH, or $H_2O$ and GSSH in the presence of GSH | $Fe_2O_3$;[16] iron chalcogenides;[17] PB;[18] MOF;[19] and metallic compounds containing Pt, Ce,[20] V, Zn,[21] Co,[21] Mn, Mo,[22] W,[23] Cu,[24] Au,[25] Ag,[26] Pd,[27] Ir,[28] Os,[29] Ru[30] | POD-like nanozymes can convert hydrogen peroxide into hydroxyl free radicals (·OH) and water; hydroxyl free radicals are the most toxic ROS, which can kill tumor cells through chemokinetic treatment, thus treating cancer |
| CAT | Catalyze $H_2O_2$ into $H_2O$ and $O_2$ | Carbon-based nanomaterials;[31,32] $Fe_3O_4$;[26] $CeO_2$;[33] $Mn_3O_4$;[34] $Co_3O_4$;[35] and metallic compounds containing Au,[36] Ag,[37] Pt,[38] Pd[27] | CAT-like nanozymes can use endogenous $H_2O_2$ to generate $O_2$, relieve hypoxia at the tumor site, and improve the therapeutic effect of RT, CTx, PDT, and SDT[39] |
| OXD | Catalyze $O_2$ into $H_2O_2$ or $\cdot O_2^-$ | $CeO_2$;[40] and metallic compounds containing Cu, Au, Ag, Pt, Ir[15] | OXD-like nanozymes can use oxygen in tumors to resynthesize $H_2O_2$ for recycling or to produce toxic superoxide anion free radicals ($\cdot O_2^-$) to further kill cancer cells |
| SOD | Catalyze $\cdot O_2^-$ into $H_2O_2$ and $O_2$ | $CeO_2$;[41] NiO;[42] metallic compounds containing Cu, Zn, Fe, Mn | SOD-like nanozymes can catalyze $\cdot O_2^-$ produced by OXD-like enzymes into $H_2O_2$ and $O_2$. On the one hand, $H_2O_2$ can generate more toxic ·OH, and on the other hand, it can alleviate tumor hypoxia |

their composition. Composite nanozymes can be classified as either purely synthetic metal-based enzymes, including metal-oxidases and monoatomic enzymes, MXene-based enzymes, or carbon-based enzymes, or as complexes that integrate both artificial and natural enzymes. Two notable natural enzymes in this context are GOx[48,49] and HRP.

In the study by Ma *et al.*, $MoS_2$ nanosheets (NSs) were decorated with Au NPs, and subsequently, Pt NPs were *in situ* grown on these nanosheets to create core–shell structured $MoS_2$–Au@Pt NPs.[50] DNA probes were then linked to the composite nanozyme through mercaptan groups, with HRP assembled into the composite nanozyme at the DNA probe level. This composite nanozyme was demonstrated to be capable of the ultra-sensitive electrochemical detection of gastric cancer-related microRNA. The presence of HRP increased the electrochemical signal of the $MoS_2$–Au@Pt NPs by approximately 10.46 times. Cui *et al.* prepared Ce and Gd dual-rare earth-doped carbon dots (Ce–Gd@CDs) using a one-step hydrothermal method, and then conjugated these with GOx through an amine reaction to form the Ce–Gd@CDs-GOx

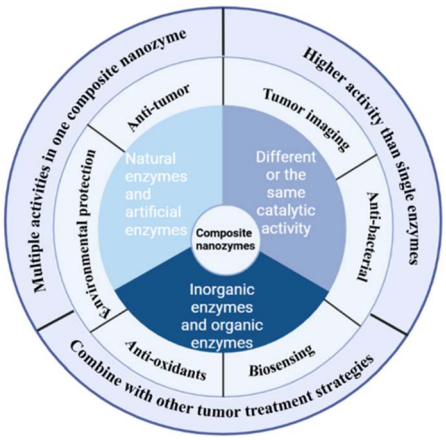


Fig. 2 Composition and application of composite nanozymes in different fields and their advantages.

complex nanozyme.[51] This composite nanozyme possessed CAT activity for alleviating hypoxia in the tumor microenvironment. It could also generate highly toxic ·OH, inducing apoptosis or necrosis in cancer cells, and with GOx catalyzing the conversion of glucose into gluconic acid and $H_2O_2$, it could deprive cancer cells of glucose, leading to the starvation of cells and ultimately cancer cell death.

There have been extensive studies on entirely synthetic composite nanozymes.[52–55] For instance, Wang *et al.* revealed that $ZnMn_2O_4$ NPs exhibited only SOD activity, while lithium-doped $LiMn_2O_4$ NPs possessed multiple enzyme activities, notably enhanced SOD activity, along with concurrent CAT and GPx activities.[56] In Zhang *et al.*'s study, platinum was deposited onto gold bipyramids (Au NBPs) using two distinct approaches: tip-specific deposition to form ATP and full-body deposition to form ACP.[57] They observed that ATP exhibited higher POD and CAT activities compared to ACP. Liu *et al.* fabricated N/P co-doped graphene quantum dots (NPGQDs) as metal-free nanozymes, which demonstrated POD activity exceeding that of traditional graphene quantum dots and graphene oxide by an order of magnitude.[58] Yang *et al.* synthesized advanced composite nanozymes of FeSA-Ir@PFNSs through the conjugation of single-atom iron (FeSA) with strained-lattice iridium metallene nanoislands.[59] The FeSA-Ir@PFNSs leveraged the POD activity of the FeSA and the photothermal effect of iridium to simultaneously generate ·OH and $^1O_2$, while also showing enhanced CAT activity.

## 2.2 Advantages of composite nanozymes

**2.2.1 Higher activity than single enzymes.** When composite nanozymes are composed of enzymes with the same catalytic function, their catalytic effect is often better than that of single enzymes. Prussian blue (PB) is a drug approved by FDA, and mesoporous Prussian blue (HPB) is often used to build cancer treatment nanodrugs.[18] Shen *et al.* found that after binding with Au NPs and Pt NPs, the CAT activity of APHPB NPs was higher than that of HPB NPs alone.[60] Also, as the concentration increased, the activity of the APHPB NPs also increased. When the concentration reached 100 μg $mL^{-1}$, their activity was nearly 45 times that of HPB NPs. After reacting with $H_2O_2$ for 10 min, the oxygen production of APHPB was more than twice that of HPB. In Wang's study, Pd@$TiO_2$, formed by binding Pd NSs and $TiO_2$, produced 6 mg $L^{-1}$ oxygen in 45 s, whereas Pd NSs needed 135 s to produce the same amount.[27]

**2.2.2 Multiple activities of composite nanozymes.** When composite nanozymes are composed of enzymes with different catalytic functions, they can achieve multiple enzyme activities or cascade catalytic effects. Taking $CeO_2$ as an example, which itself has CAT and SOD activities. Wang doped Cu into $CeO_2$ NPs, and increased the $Ce^{3+}/Ce^{4+}$ ratio of $CeO_2$. Subsequently, the POD activity of the composite nanozyme was found to be increased, resulting in better cancer inhibition rates and reduced toxicity to healthy tissues.[24] RuCu NSs synthesized by Yang not only demonstrated POD activity to produce ·OH, but also SOD and GPx activities.[30] $\cdot O_2^-$ radicals were converted into $H_2O_2$ under the catalysis of RuCu NSs, increasing the concentration of $H_2O_2$ in the TME, and leading to the production of more ·OH. At the same time, the nanosheets consumed GSH to prevent ·OH from being consumed by GSH. The cascade catalytic reaction with multiple enzyme activities resulted in a much higher efficiency of the composite nanozyme in catalyzing the Fenton reaction than the single enzyme and natural enzyme ($K_{cat}/K_m$ = 83.3 $m^{-1}$ $s^{-1}$).

**2.2.3 Combination with other cancer treatment strategies.** In addition to improving catalytic ability, composite nanozymes have also been given other abilities that can be used in combination with other therapies. For instance, PB alone has a weak photothermal conversion ability, but He *et al.* found that PB NPs doped with $Co^{2+}$ and $La^{3+}$ exhibited stronger photothermal ability, and the solution could be heated to 43 °C within 10 min, resulting in a photothermal conversion rate of 30.0%.[61] This nanozyme was then used in combination with PTT to greatly inhibit tumor growth in mice. Some composite nanozymes are also given magnetism, which can be used for magnetic targeting or magnetic resonance imaging (MRI) to achieve integrated diagnosis and treatment. There are reports that PB NPs can be used as a T1 weighted contrast agent for MRI, but its ability to judge tumors is still weak. Nie *et al.* engineered a $Cu_{0.5}Mn_{0.5}Fe_2O_4$ (CMF) nanozyme that was characterized by an abundance of catalytically active sites on its surface, which possessed both GPx and POD activities. This nanozyme could dismantle the antioxidant defenses of tumors and generate a substantial quantity of ROS. In addition, its CAT and OXD activities facilitated the continuous generation of oxygen and superoxide anions, leading to an overproduction of ROS. Leveraging the superparamagnetic properties of Mn and Fe, this nanozyme demonstrated superior T1–T2 dual-mode MRI capabilities both *in vivo* and *in vitro*, enabling the precise delineation of tumor regions.[62]

Other than the aforementioned advantages, some composite nanozymes can also allow reducing production costs, such as doping non-noble metal nanoparticles (Cu, Mn) into precious metal nanozymes (Au, Ru). This approach not only lowers raw material expenses, but can also improve catalytic efficiency. Furthermore, some composite nanozymes can reduce the toxicity of single nanozymes and have higher levels of biosafety and bioavailability.

## 3. Synthesis of composite nanozymes

Composite nanozymes can be synthesized through solvent/hydrothermal doping, chemical deposition, covalent bonding, *in situ* growth, and other methods. Due to their excellent catalytic performance and other endowed properties, composite nanozymes are usually designed for use in combination with other treatment methods, such as PDT, PTT, SDT, ST,[63] or CTx. In addition, composite nanozymes have also been designed as imaging probes or nano-platforms for diagnosis and treatment. However, this article is only focused on the application of composite nanozymes in cancer treatment. Table 3 summarizes and provides examples of the commonly used synthesis methods and the design of nanozymes in this field.

### 3.1 One-step solvent/hydrothermal synthesis

One-step solvent/hydrothermal synthesis is a simple and effective synthesis method that involves doping metal-based nanozymes into composite nanozymes with more catalytic capabilities. Yin *et al.* used a one-step solvent method to dope Ce into $ZnCo_2O_4$ NPs.[21] The oxygen vacancies, superoxide radicals, and electron transfer of $Ce/ZnCo_2O_4$ jointly promoted the enhancement of the POD and OXD activities. Based on the dual enzyme-like activity of $Ce/ZnCo_2O_4$, $H_2O_2$ and GSH could be quickly and conveniently detected. Zhong *et al.* synthesized uniform $PtCu_3$ nanocages using a one-pot solvothermal method (Fig. 3A).[64] After PEG synthesis, the synthesized $PtCu_3$-PEG nanocages could not only serve as a new sound sensitizer to generate ROS under ultrasonication (US), but could also serve as POD nanozymes to catalyze the decomposition of $H_2O_2$ into ·OH. At the same time, $PtCu_3$ PEG nanocages, as GSH-Px nanozymes, could accelerate the process of GSH depletion in the presence of oxidizing molecules ($H_2O_2$, $O_2$). Wang *et al.* designed a simpler and environmentally friendly one-pot method to synthesize a $Au_2Pt$ nanozyme at room temperature (Fig. 3B).[25] Here, L-proline was introduced as a chelating agent to slow down the kinetics of the

Table 3 Summary of the design and synthesis of composite nanozymes

| Synthesis method | Composite nanozyme system | Enzyme mimic | Enzyme/enzyme mimic activity | Combination therapy |
|---|---|---|---|---|
| Solvent/hydrothermal synthesis | CCCs[24] | Cu–$CeO_2$ | POD, CAT, SOD | CTx |
| Solvent/hydrothermal synthesis | $Ce/ZnCo_2O_4$ [21] | $Ce/ZnCo_2O_4$ | POD, OXD | — |
| Solvent/hydrothermal synthesis | Ox-POM@Cu[22] | Ox-POM@Cu | GSH-PX, CAT | PTT, CDT |
| Solvent/hydrothermal synthesis | $PtCu_3$-PEG[64] | $PtCu_3$ | POD, GSH-PX | SDT, CDT |
| Solvent/hydrothermal synthesis | Cu–$CuFe_2O_4$/DOX[65] | Cu–$CuFe_2O_4$ | POD, GSH-PX | SDT, CDT, CTx |
| Solvent/hydrothermal synthesis | RuCu NSs[30] | RuCu | POD, SOD, GSH-PX | CDT |
| Solvent/hydrothermal synthesis | MnWOx-PEG[66] | MnWOx | POD, GSH-PX | SDT |
| Solvent/hydrothermal synthesis | PtFe@$Fe_3O_4$ [67] | PtFe@$Fe_3O_4$ | POD, CAT | PTT |
| One-step synthesis | $Au_2Pt$-PEG-Ce6 [25] | $Au_2Pt$ | POD, CAT | PTT, PDT, CDT |
| Solvent/hydrothermal synthesis and coat | Co/La-PB@MOF-199/GOx[61] | Co/La-PB@MOF-199 | POD, CAT, GOx | PTT, CDT |
| Solvent/hydrothermal synthesis | CMO-R@4T1 [68] | CMO (Cu-doped MoOx) | POD, OXD, NADH-oxidase | PTT, immunotherapy |
| Chemical deposition | Au NBP/Pd[69] | Au NBP/Pd | POD | PTT, PDT |
| Chemical deposition | CuS@$CeO_2$ [70] | CuS@$CeO_2$ | CAT | PTT, RT |
| Liquid-phase deposition | PTZCs[27] | Pd@$TiO_2$ | CAT | PTT, PDT |
| Vacuum metal sputter deposition | Pt–CuS–P-TAPP[71] | Pt–CuS | CAT | PTT, SDT |
| Vacuum metal sputter deposition and reduction | HPT-DOX[72] | Pt–$TiO_2$ | CAT | SDT |
| *In situ* growth | Ce6–Au–Pt@HPBs[60] | Au–Pt@HPBs | CAT | PDT |
| *In situ* growth and thermal decomposition | $MnFe_2O_4$@MOF@PEG[73] | $MnFe_2O_4$@MOF | GSH-PX, CAT | PDT |
| *In situ* growth | $MnO_2$@PtCo[74] | $MnO_2$@PtCo | CAT, OXD | — |
| *In situ* growth | HAMF[75] | HMSN@Au@$MnO_2$ | CAT, OXD | PDT |
| *In situ* growth | Pt–carbon[76] | Pt–carbon | CAT | PTT, PDT |
| *In situ* growth | ICG/Au/Pt@PDA–PEG[77] | Au–Pt | POD, CAT, OXD | PTT, PDT, ST |
| *In situ* growth and adsorption | P@Pt@P-Au-FA[78] | P@Pt@P–Au | CAT, OXD | PDT, ST |
| *In situ* growth and template method | PDAP-ICG-Pt[79] | PDAP–Pt | GSH-PX, CAT | PDT |
| | CM-MMNPs[80] | MOF-$MnO_{2\#}$ | CAT | PDT |
| *In situ* growth and etching | $Ti_3C_2Tx$–Pt-PEG[81] | $Ti_3C_2Tx$–Pt | POD | PTT |
| Solvent and hydrothermal synthesis, *in situ* growth | FAB NPs[26] | $Fe_3O_4$/Ag/$Bi_2MoO_6$ | POD, GSH-PX, CAT, SOD | PTT, PDT, CDT |
| Template method | HMCGP[82] | HMCu$O_2$–GOD | CAT, GSH-PX, OXD | PTT, PDT, ST |
| Template method and reduction | Pt@HCS-Ce6 NPs[83] | Pt@HCS | POD, OXD | PDT |
| Template method | FePc/HNCSs[84] | FePc/HNCS | POD, CAT | PTT, PDT |
| Solvothermal galvanic replacement | Os–Te NRs[29] | Os–Te | POD, CAT, SOD | PTT, PDT |
| Inverse microemulsion polymerization | RONS[85] | Fc@Gox | OXD, GOx | CDT |
| Thermal decomposition | CFS@PF-CPT[17] | $CuFeS_2$ | POD, CAT, GSH-PX | PTT, PDT, CDT, CTx |
| Loading and etching | DFMC[86] | $Fe_3O_4$–Mn | POD, GSH-OXD | CDT |

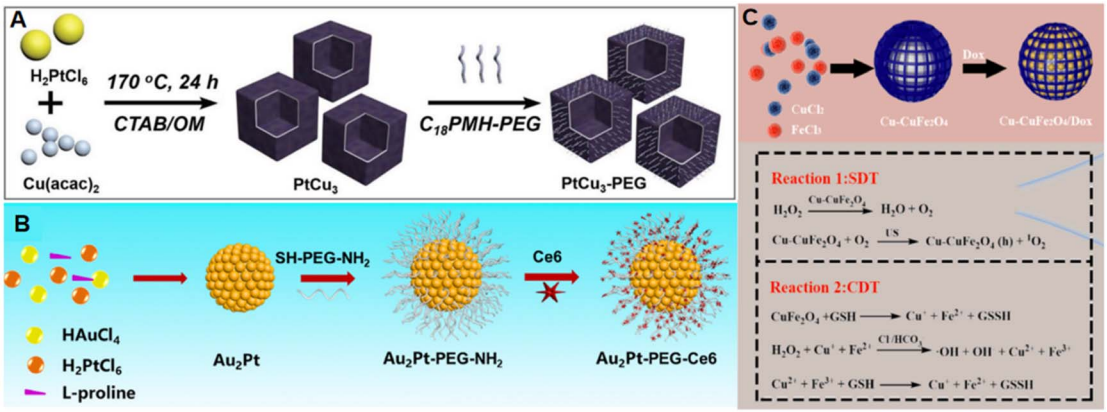


Fig. 3 A) Schematic of the synthesis of $PtCu_3$-PEG. This figure has been adapted/reproduced from ref. 64 with permission from WILEY, copyright 2019. (B) Schematic of the synthesis of Cu–$CuFe_2O_4$/DOX. This figure has been adapted/reproduced from ref. 25 with permission from ELSEVIER, copyright 2020. (C) Schematic of the synthesis of AuPt-PEG-Ce6. This figure has been adapted/reproduced from ref. 65 with permission from ELSEVIER, copyright 2022.

reduction reaction. Through the interaction of thiol groups with Au and Pt atoms, SH-PEG–$NH_2$ was coupled to the surface of $Au_2Pt$. Finally, Ce6 was connected to the surface of $Au_2Pt$ PEG–$NH_2$ through an acylation reaction. After combining with Ce6, the nanozymes could not only simulate POD and CAT enzymes, but also combine with PTT and PDT to achieve better therapeutic effects. Similarly, Gong *et al.* synthesized a Cu-doped MOF (Cu–$CuFe_2O_4$) using a one-step hydrothermal method (Fig. 3C) and loaded this with the chemotherapy drug DOX and sonosensitizer agent Ce6.[65] The nanozyme, while also possessing a catalytic function, could be combined with SDT and CTx for anti-cancer application.

### 3.2 Deposition

The deposition method is an effective synthesis method for obtaining composite nanozymes, and the deposition position of nanoparticles can also be selected. Yu *et al.* selectively deposited Pd NPs onto the tip of Au NBPs (Fig. 4A), and synthesized well-defined anisotropic photonanozymes, which exhibited peroxidase-like properties that were enhanced by 1.5 times under light excitation.[69] At the same time, Au and Pd NPs exhibited strong PDT and PTT abilities. Liang *et al.* synthesized partially Pt deposited CuS Janus NPs through a vacuum metal sputter deposition method.[71] The addition of Pt increased the temperature of CuS NPs by 30 °C after being irradiated with 808 nm laser. The hollow structure and negative surface potential of the Pt–CuS Janus NPs promoted the loading of the sound-sensitive agent tetra-(4-aminophenyl)porphyrin (TAPP). Triggering of the TAPP release mode by US was found to be particularly helpful for the cavitation effect of US (Fig. 4B), while at the same time, $O_2$ could be generated *in situ* to promote PTT and SDT to kill cancers.

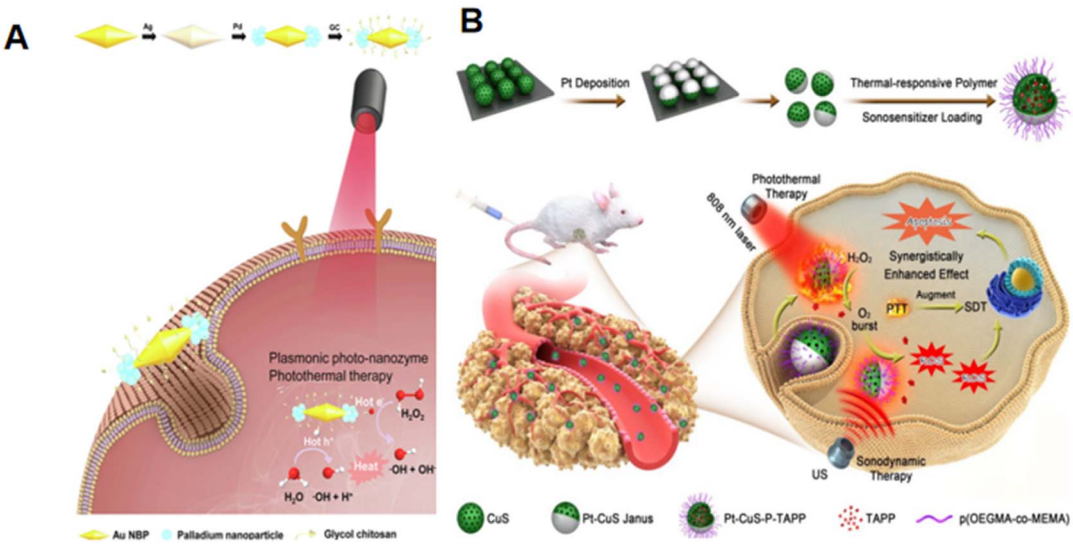


Fig. 4 (A) Schematics of Au NBP/Pd synthesis, and *in vitro* plasma photo nuclease therapy for cancer based on POD activity and photothermal effect under near-infrared light irradiation. This figure has been adapted/reproduced from ref. 69 with permission from ELSEVIER, copyright 2021. (B) Schematics of Pt–CuS Janus NPs synthesis, and the CAT-like activity and the combination of PTT and SDT for cancer treatment. This figure has been adapted/reproduced from ref. 71 with permission from the American Chemical Society, copyright 2019.

### 3.3 *In situ* growth

Metal nanoparticles, especially Au and Pt NPs, can be combined in larger nanoparticle platforms by reducing metal salt solutions in mixed solutions. Cold $NaBH_4$ is often used to synthesize composite nanozymes in the *in situ* growth method. For example, Shen *et al.*[60] mixed $HAuCl_4 \cdot 4H_2O$ and $H_2PtCl_6 \cdot 6H_2O$ with etched HPB NPs, and then slowly added cold $NaBH_4$ solution to the mixture. After stirring, APHPBs with Au NPs and Pt NPs on the surface were synthesized. APHPBs loaded with Ce6 could catalyze $H_2O_2$ to generate oxygen, which in turn generated $^1O_2$ under the action of Ce6, enhancing the therapeutic effect of PDT. Similarly, in Chen *et al.*'s study,[75] $HAuCl_4$ was adsorbed on the surface of pre-synthesized mesoporous silica nanoparticles (HMSNs) with the help of cold $NaBH_4$ and then grown into AuNPs. Subsequently, the $MnO_2$ shell was covered by the *in situ* reduction, and finally, 4-FM, a TADF fluorescein derivative, was connected to the surface of the nanozyme through an amide reaction. It was found that $H_2O_2$ could be catalyzed into $O_2$ by $MnO_2$ in the HAMF nanozyme to alleviate TME hypoxia. Meanwhile, glucose was oxidized into gluconic acid and $H_2O_2$ by Au to promote cell starvation treatment and $H_2O_2$ circulation. At the same time, the generation of $O_2$ could enhance PDT (Fig. 5A).

Polydopamine (PDA) has excellent photothermal conversion efficiency and multifunctional reactivity, making it often selected as a photothermal agent (PTA). At the same time, PDA can serve as a carrier for nanozymes and photosensitizers. In the work of Ciou *et al.*, PDA was used as both a carrier for nanozymes and as a reducing agent, as it can form complexes with metal ions.[77] $HAuCl_4$ and $K_2PtCl_6$ were reduced to Au NPs and Pt NPs attached to the surface of PDA. Meanwhile PEG was connected to Au/Pt@PDA NPs through covalent interactions, and ICG was subsequently connected to the Au/Pt@PDA–PEG NPs through π–π interactions (Fig. 5B). The Pt NPs in the final synthesized nanozymes possessed the catalytic abilities of POD and CAT, catalyzing $H_2O_2$ into hydroxyl radicals and oxygen, respectively, and then glucose was oxidized into gluconic acid by $O_2$, while $H_2O_2$ could be re-generated under the OXD activity of Au NPs, thereby allowing $H_2O_2$ circulation to be achieved. Under an NIR laser, a large amount of was heat generated for photothermal therapy, because of the ICG and PDA. In addition, singlet oxygen was generated in large quantities under the action of ICG, which, together with the hydroxyl radicals, induced cell apoptosis and promoted photodynamic therapy.

### 3.4 Template method

Hollow materials are usually synthesized through the template method, whereby nanozyme layers (such as metal oxides or

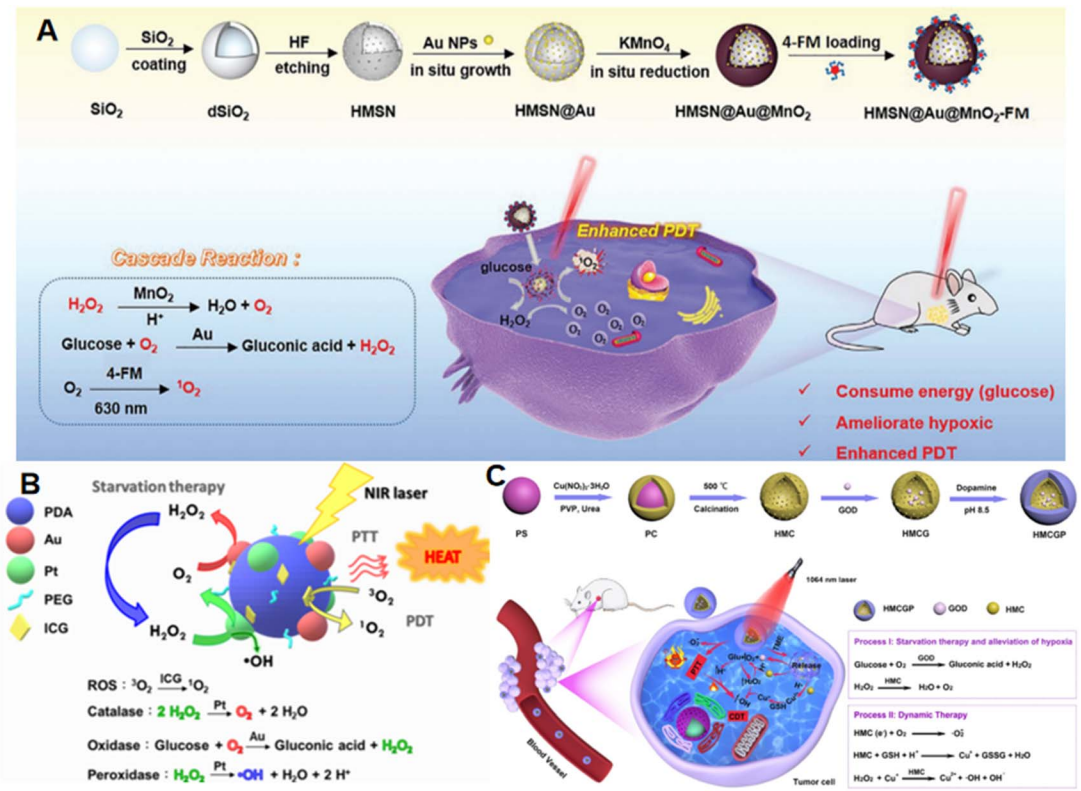


Fig. 5 (A) Schematic of the synthesis process of HMSN@Au@$MnO_2$-FM NPs and the mechanism for relieving cancer hypoxia and improving PDT by nanozyme-catalyzed cascade reactions. This figure has been adapted/reproduced from ref. 75 with permission from WILEY, copyright 2021. (B) Schematic for the proposed mechanism of ICG/Au/Pt@PDA–PEG NPs for the cooperative effect of ST/PTT/CDT. This figure has been adapted/reproduced from ref. 77 with permission from the American Chemical Society, copyright 2021. (C) Schematic of the synthesis of HMCGP and the mechanism of HMCGP for the starvation therapy-promoted alleviation of cancer hypoxia and combined photothermal–catalytic therapy by cascade enzymatic reactions. This figure has been adapted/reproduced from ref. 82 with permission from the American Chemical Society, copyright 2022.

carbon nanolayers) are deposited or reduced on hard templates ($SiO_2$ is often used as a template), and then sacrificed by etching or by applying a high-temperature method to leave mesoporous nanozyme particles. Other active nanozymes may then be connected to them through different methods to form composite nanozymes.

Polystyrene NPs were used as a template by Wang and colleagues,[82] where, due to their opposite charges, CuO was adsorbed and reduced on the surface of the polystyrene NPs, followed by calcination at 500 °C to form HMC NPs. GOD was then loaded into the cavities and mesopores of HMC NPs to obtain GOD–CuO (HMCG) nanocomposites. Finally, PDA was coated on the surface of HMCG to improve its biosafety and bioavailability (Fig. 5C). After entering the cancer site, the nanozymes could be released under laser irradiation, playing the roles of CAT and OXD, respectively, and producing oxygen to alleviate TME hypoxia, while consuming glucose to promote starvation treatment, replenishing $H_2O_2$, or producing toxic ROS, and oxidizing GSH to prevent ROS from being disproportionated. Thus, the therapeutic effect of CDT could be greatly improved, and then combined with PTT to kill cancer cells.

### 3.5 Other methods

GOx was used as a template by Liu *et al.*, and a nanozyme containing arginine and ferrocene was synthesized by reverse microemulsion polymerization.[85] This nanozyme could consume glucose, produce nitric oxide and highly toxic hydroxyl radicals and superoxide anions. Then, a peroxynitrous acid radical anion was generated through the reaction between NO and $\cdot O_2^-$, thus stimulating reactive oxygen species and nitrogen (RONS) radical storms to effectively eradicate cancer cells *in vitro* and *in vivo*. Os is one of the group 8 elements, and nanostructures based on Os may have potential in various applications, including biomedical fields. However, it is difficult to synthesize Os NPs using traditional Ag nanotemplates under any conditions, thus Kang *et al.* tried to use TeNRs as templates to conduct solvothermal current displacement, and were able to finally successfully prepare OsTeNRs with both POD, CAT, SOD, and OXD activities.[29]

## 4. Factors affecting the catalytic activity of nanozymes

The catalytic efficacy of nanozymes is influenced by a multitude of parameters, including but not limited to, the morphological attributes, dimensional characteristics, elemental constituency, surface functionalization, and environmental perturbations, such as photic irradiation, sonication, thermal variations, and pH fluctuations.[11,87,88] These factors can exert a significant control over the catalytic behavior of nanozymes and must be meticulously considered in the strategic design and fabrication of composite nanozyme systems to optimize their performance in biomedical applications.

### 4.1 Dimensions

The dimensions of nanoparticles significantly influence their catalytic activity due to the direct correlation between the particle size and the number of surface-active sites. The distribution and density of these sites on the nanoparticle's surface are pivotal in determining the catalytic activity. Nanoparticles with smaller sizes demonstrate enhanced catalytic activity owing to their increased surface-area-to-volume ratio, which escalates the likelihood of substrate interaction. Precise synthetic manipulation of the diameter of nanoparticles allows fine-tuning their catalytic properties. In the case of $CeO_2$ NPs, it has been established that a reduction in nanoparticle size is accompanied by an enlargement of the specific surface area, leading to an increased exposure of active sites and a heightened probability of substrate contact. Additionally, the downsizing of nanoparticles is linked to a higher density of surface oxidation vacancies, which can effectively accelerate $Ce^{3+}/Ce^{4+}$ redox cycling, thereby augmenting the catalytic activity.[89] For this reason, Tang *et al.* integrated ultra-small $CeO_2$ NPs with core–shell-structured Au@Pt NPs to fabricate $CeO_2$/Au@Pt-PEG composite nanozymes, which demonstrated enhanced POD enzyme activity and augmented the generation of ROS and the efficacy of CDT in tumor therapy.[90]

### 4.2 Morphology

The catalytic activity of nanozymes is influenced by their morphology. Varying shapes, such as nanorods, nanowires, nanospheres, and nanofibers, possess distinct crystal facets, exposing different dangling bonds and atomic arrangements, which may increase the number of active sites, thereby enhancing the activity of the nanozymes. Qian *et al.* synthesized three morphologically distinct magnetite nanozymes (MNZs): spherical (SMNZ), ellipsoidal (EMNZ), and flaky (FMNZ). They observed that FMNZ exhibited the highest POD activity under weakly acidic conditions (pH 5.0), with a specific activity reaching 2.376 U $mg^{-1}$, significantly outperforming SMNZ and EMNZ. Moreover, FMNZ demonstrated a faster and greater release of iron ions across all pH conditions, contributing to its enhanced POD activity. Similarly, FMNZ showed higher GPx activity compared to the other two MNZs tested. The flaky morphology also facilitated better internalization of the nanozyme by cancer cells. *In vivo* experiments revealed that FMNZ accumulated more in tumor tissues than SMNZ and EMNZ did.[91]

### 4.3 Composition

The composition of nanozymes is a critical factor influencing their activity. Composite nanozymes often exhibit higher catalytic activity than their single counterparts. Luo *et al.* constructed an Au@Pd composite nanozyme, which demonstrated a $K_m$ slightly higher than that of natural HRP, while its $V_{max}$ was significantly higher than that of both HRP and Au NPs.[92] When the same nanozyme base was doped with different metal elements to form composite nanozymes, their catalytic efficiencies varied. Nguyen *et al.* doped various metal elements into

cerium oxide nanoparticles, creating M–$CeO_2$ NPs (where M represents a metal element, including Fe, Co, Ni, Cu, and Zn). They calculated the peroxidase activity of the different NPs and found significant differences in their catalytic activity depending on the doped element. Notably, Co–$CeO_2$ NPs showed the highest enzyme activity, which was 627.5 times greater than that of $CeO_2$ NPs.[93] Changes in the valence state of the same metal nanozyme can also lead to alterations in catalytic action. For example, Zeng *et al.* synthesized four vanadium oxide nanozymes (Vnps-I, Vnps-II, Vnps-III, Vnps-IV) using a simple method, with the primary distinction among these Vnps being the ratio of $V^{4+}$ to $V^{5+}$. Vnps-III, containing a lower vanadium valence state ($V^{4+}$), exhibited good POD and OXD activities, while Vnps-I, containing a higher vanadium valence state ($V^{5+}$), possessed CAT activity.[94]

### 4.4 Surface modification

The surface modification of nanozymes can enhance their biocompatibility or enable them to achieve targeted localization. Since the majority of catalytic reactions occur on the surface of NPs, surface modification can not only improve the biocompatibility, aqueous dispersibility, and biological targeting capabilities of nanozymes but also influence their catalytic activity. Surface alterations encompass the incorporation of functional groups, inorganic ions, minute particles, and polymers, thereby modulating the characteristics of the nanozymes through the modification of their surface chemistry. For instance, He *et al.* synthesized Pt NPs decorated with carboxymethyl chitosan (CC–Pt NPs) and observed that these CC–Pt NPs exhibited a superior dispersion and maintained stable catalytic activity across a broader range of temperatures and pH values. Moreover, they demonstrated stronger ascorbate oxidase activity compared to unmodified Pt NPs.[95]

### 4.5 Environmental factors

The catalytic activity of nanozymes is not only determined by their intrinsic properties but may also be influenced by environmental stimuli, including exogenous and endogenous factors. Exogenous stimuli, such as light irradiation, ultrasound, temperature, and magnetism, can modulate the activity of nanozymes. Extensive research has revealed that certain noble metal nanozymes exhibit excellent photothermal conversion efficiency. Under NIR-II irradiation, such nanozymes convert light energy into heat, whereby the subsequent increase in temperature enhances the catalytic activity of the nanozymes.[87] For instance, Au NPs are widely studied nanozymes with photothermal properties.[57,90,96,97] Carbon-based nanozymes also possess photothermal characteristics. Feng *et al.* developed a mesoporous carbon nanozyme (MC-PEG) and observed that under NIR-II irradiation, it significantly increased the temperature of tumor cells and generated more ·OH, thereby demonstrating more effective and sustained glutathione GPx activity and more potent POD activity compared to graphene oxide nanoparticles.[98] In another investigation, Saravanan *et al.* linked photothermal 2D material $MoS_2$ nanoflowers with $CeO_2$ NPs. Upon NIR-II irradiation, the temperature rose, which enhanced the POD enzyme activity of the $CeO_2$ NPs.[99] Recently, Dong *et al.* reported that US could significantly enhance the POD simulated catalytic activity of $CaF_2$ nanozymes, and by increasing the collisions and interaction probability between $H_2O_2$ and the catalytic center, they could finally achieve efficient anti-tumor effects in 4T1 breast cancer and H22 liver cancer animal models.[100]

Endogenous stimulation, primarily referring to pH and ROS within the TME, can play a significant role in modulating the activity of nanozymes. Among the four vanadium oxide nanozymes discussed above in Section 4.3, Vntp-III and VNTP-IV displayed heightened POD activity under acidic conditions (pH 6.0), effectively generating ROS for tumor treatment. Vnps-I exhibited more robust CAT activity than the other nanozymes tested under standard conditions and could maintain this activity across both pH 7.4 and pH 6.0, aiding amelioration of the hypoxic solid tumor environment.[94] In a related study, Chen *et al.* illustrated that iron oxide nanoparticles (IONPs) presented POD activity under acidic conditions and CAT activity under neutral conditions (pH 7.4). They also demonstrated that these nanozymes retained high catalytic activity in the TME while being non-toxic to healthy tissues.[101]

## 5. Application of composite nanozymes in cancer treatment

Composite nanozymes fight cancer by producing oxygen, producing different reactive oxygen species, consuming glucose, or their cascades, or in combination with other therapies to overcome cancer. Table 4 summarizes some applications of composite nanozymes in different cancer treatments.

### 5.1 Different approaches to the treatment of cancer

**5.1.1 Composite nanozymes as nanomedicines for cancer therapy.** The POD or OXD activity of composite nanozymes enables them to generate toxic ROS, which can lead to apoptosis in cancer cells and inhibit tumor growth. Enzymes with GPx activity can consume GSH, thereby reducing the quenching of ROS and promoting apoptosis in cancer cells. This therapeutic approach is often referred to as CDT. Composite nanozymes with GOx activity can deplete glucose in the tumor region, reducing the tumor's energy supply, leading to tumor "starvation". Therefore, nanozymes with such catalytic activities can be used directly as nanomedicines for cancer treatment. Li *et al.* synthesized a bismuth–manganese core–shell-structured nanoflower loaded with glucose oxidase (BDS–GOx@MnOx NPs), whose MnOx shell could react with $H_2O_2$, reduce $Mn^{3+}$ to $Mn^{2+}$, and generate ·OH through a Fenton-like reaction, which can destroy tumor cells. Subsequently, $Mn^{3+}$ was reduced to $Mn^{2+}$ by GSH, while consuming GSH and leading to the accumulation of GSSG, further weakening the antioxidant capacity of tumor cells. Concurrently, the release of GOx enhanced the ST effect. Due to the presence of Bi and Mn, this nanozyme could also be used to enhance CT and MR imaging for improving the diagnostic accuracy of tumors.[48] Dong *et al.* constructed a transition metal-doped hollow ceria nanozyme (PHMZCO-AT NPs) that could disrupt the homeostasis of $H_2O_2$

 

Table 4 Application of composite nanozymes in different cancer treatments

| Cancer type | *In vitro* | *In vivo* | Nanozyme | Applications |
|---|---|---|---|---|
| Breast cancer | 4T1 | 4T1 | BDS–GOx@MnOx[48] | CDT, ST |
| Breast cancer | 4T1 | 4T1 | PHMZCO-AT[102] | CDT |
| Breast cancer | 4T1 | 4T1 | APHPBs[60] | PDT |
| Breast cancer | 4T1 | 4T1 | Co/La-PB@MOF-199/GOx[61] | CAT, PTT, ST |
| Breast cancer | 4T1 | 4T1 | CMO-R@4T1 [68] | PTT, immunotherapy |
| Breast cancer | 4T1 | 4T1 | FAB NP[26] | CDT, PDT, PTT |
| Breast cancer | 4T1 | 4T1 | P@Pt@P-Au-FA[78] | PDT, ST |
| Breast cancer | 4T1 | 4T1 | $PtCu_3$-PEG[103] | CDT, SDT |
| Breast cancer | 4T1 | 4T1 | RuCu NSs[30] | CDT |
| Breast cancer | 4T1 | 4T1 | FePc/HNCSs[84] | PDT, PTT |
| Breast cancer | 4T1 | 4T1 | NC@GOx[63] | CDT, PTT, ST |
| Breast cancer | MCF-7 | 4T1 | $Fe_3O_4$@$MnO_2$ [104] | ST, RT |
| Breast cancer | MCF-7 | MCF-7 | PDAP-ICG-Pt[79] | PDT, PTT |
| Breast cancer | MCF-7 | — | Cu–$CuFe_2O_4$ [65] | CDT, SDT, CTx |
| Breast cancer | MDA-MB-231 | MDA-MB-231 | CCCs[24] | CAT, CTx |
| Cervical cancer | HeLa | U14 | $Au_2$Pt-PEG-Ce6 [25] | CDT, PDT, PTT |
| Cervical cancer | HeLa | U14 | HMCGP[82] | CDT, PTT, ST |
| Cervical cancer | HeLa | — | CM-MMNPs[80] | PDT |
| Cervical cancer | HeLa | 4T1 | $MnFe_2O_4$@MOF[73] | PDT |
| Cervical cancer | HeLa | 4T1 | PTZCs[27] | PDT, PTT |
| Colon cancer | CT26 | CT26 | $Au_1Pd_3$ [62] | CDT |
| Colon cancer | CT26 | CT26 | PCPT[71] | PTT, SDT |
| Colon cancer | CT26 | CT26 | HCS@Pt–Ce6 [83] | PDT |
| Colon cancer | CT26 | CT26 | Pt–carbon[76] | CDT, PDT |
| Colon cancer | CT26 | CT26 | DFMC[86] | CDT |
| Melanoma | B16F1 | — | ICG/Au/Pt@PDA–PEG[77] | CDT, PDT, PTT |
| Melanoma | B16F1 | — | CFS@PF[17] | CDT, PDT, PTT, CTx |
| Liver cancer | HepG2 | HepG2 | MnO–N/C[105] | CDT, PTT |
| Liver cancer | RIL-175 | RIL-175 | OsTeNRs[29] | CDT, PDT, PTT, CTx, immunotherapy |
| Liver cancer | HepG2 | HepG2 | CuS@$CeO_2$ [70] | PTT, RT |
| Glioblastoma | U87MG | U87 MG | Au NBP/Pd[69] | CDT, PTT |
| Glioblastoma | U87MG | — | $MnFe_2O_4$/C[106] | PTT |
| Pancreatic cancer | SW1990 | SW1990 | PtFe@$Fe_3O_4$ [67] | CDT, PTT |
| Non-small cell lung cancer | A549 | A549 | Arg/Fc@GOx/HA[85] | CDT, ST |

within tumor cells by modulating SOD activity, POD activity, and inhibiting CAT activity, thereby enhancing the efficacy of CDT.[102] Meng *et al.* developed composite nanozymes with varying Au/Pd ratios that could mimic neutrophil activity, generating highly oxidative species, such as hypochlorous acid (HClO) and $^1O_2$, through a cascade reaction of SOD and myeloperoxidase (MPO), to kill microbes or tumor cells. In their study, they found that $Au_1Pd_3$ NPs exhibited the highest SOD and MPO activities, inhibiting tumor growth through the SOD–MPO cascade catalytic reaction.[107]

**5.1.2 Combined treatment by composite nanozymes and light-based therapy.** Phototherapy has emerged as a significant focus in recent cancer treatment research due to its direct targeting capability and non-invasive nature. PDT is a form of phototherapy where three parameters directly influence the therapeutic outcome: light exposure, photosensitizer, and oxygen. Consequently, the substantial hypoxia in tumor tissues significantly limits the efficacy of PDT. However, the CAT activity of nanozymes can generate oxygen from $H_2O_2$ in the TME, which can alleviate hypoxia and enhance the tumor-killing effect of PDT.[108] Based on this principle, Han and colleagues developed a composite nanozyme ($MnFe_2O_4$/C@Ce6 NPs) loaded with the photosensitizer Ce6. This nanozyme exhibited significant CAT enzyme activity, and under hypoxic conditions, it was found to generate a substantially higher level of ROS than Ce6 alone, leading to a remarkable killing effect on cancer cells.[106]

PTT is an alternative modality of phototherapy, in which photosensitizers convert light energy into heat, leading to increased blood circulation in the tumor region. This temperature elevation enhances the penetration and effectiveness of nanozymes and can cause the demise of cancer cells due to hyperthermia. The combination of PTT with nanozymes to generate ROS for tumor treatment is a promising therapeutic approach. In the study by Hu *et al.*, a manganese oxide/nitrogen-doped carbon composite nanozyme (MnO–N/C NPs) with photothermal conversion capability was developed. Upon irradiation with an 808 nm near-infrared laser, the POD, OXD, and CAT activities of MnO–N/C NPs were accelerated. The high temperature, in conjunction with the production of multiple ROS, led to apoptosis in cancer cells. Moreover, these nanozymes possessed T1-weighted MRI capabilities, enabling the MRI-guided efficient photothermal and enhanced catalytic synergistic treatment of tumors in mice.[105]

**5.1.3 Combined treatment by composite nanozymes and SDT.** Given the limited penetration depth of light and the

potential for irreversible damage to surrounding normal tissues due to the high temperatures, US, which possesses a greater penetration depth and higher safety, has attracted much attention for its use in SDT for treating tumors. Similar to PDT, the efficacy of SDT is contingent upon three core elements: ultrasound, sonosensitizers, and oxygen. Consequently, SDT is typically employed in conjunction with nanozymes that exhibit CAT or SOD activity to alleviate hypoxia in the TME, thereby enhancing the therapeutic outcome of SDT. Furthermore, SDT can be integrated with other active nanozymes.[109] For instance, Zhou *et al.* constructed a PdPt composite nanozyme (PdPt@GOx/IR780 NPs) that was conjugated with both GOx and the sonosensitizer IR780. This nanozyme could not only generate oxygen to ameliorate hypoxia but also consumed glucose, cyclically producing $H_2O_2$, leading to an enhancement in the efficacy of SDT while also promoting the effects of ST.[110]

**5.1.4 Combined treatment by composite nanozymes with RT and CTx.** RT and CTx are conventional modalities for cancer treatment. Radiotherapy (RT) is a tumor-treatment method based on the direct interaction of X-rays with cellular DNA, which can cause damage or indirectly react with $H_2O_2$ to generate ROS. However, the efficacy of RT is often reduced by tumor hypoxia and radioresistance, while it can also show pronounced adverse side effects, thus prompting the need to modify and improve traditional therapeutic approaches. In this regard, Yin *et al.* engineered a composite nanozyme (BMBs), possessing POD, GPx, and NADPH dehydrogenase activities. By depleting GSH and NADPH, they found that the BMBs could attenuate the ferroptosis defense system within tumor cells, suppressing the activity of GPX4 and FSP1 in particular. Concurrently, excessive ROS production could disrupt the redox equilibrium of tumors, triggering death mechanisms. The Bi component within the BMBs nanozyme, characterized by its high atomic number, could effectively absorb X-rays, enhancing the energy deposition of X-rays and further augmenting the cytocidal effects of radiotherapy on tumors.[111]

DOX is a potent and highly popular chemotherapeutic agent; however, it is commonly associated with cardiotoxicity. To mitigate the cardiac side effects of this drug, Xing *et al.* developed a novel auric ruthenium (AuRu) bimetallic cluster nanozyme conjugated with atrial natriuretic peptide (ANP), termed ATBMzyme. In co-administration studies, this enzyme has been shown to target the heart, demonstrating robust antioxidant activity within cardiomyocytes, as well as being able to effectively scavenge free radicals, and reduce DOX-induced ferroptosis in cardiac cells. Additionally, ATBMzyme has been observed to alleviate DOX-induced hepatotoxicity and nephrotoxicity without compromising the therapeutic efficacy of DOX against tumors.[112]

### 5.2 Application of composite nanozymes for the treatment of different cancers

**5.2.1 Breast cancer.** Breast cancer has replaced lung cancer as the most common cancer in the world. The number of patients suffering from breast cancer accounts for 12.5% of the total number of cancer patients and 25% of the total number of women suffering from cancer.[113] The current treatment for breast cancer includes targeted therapy, hormone therapy, radiation therapy, and surgery.[114] Common CTx drugs for breast cancer include cyclophosphamide, paclitaxel, doxorubicin, gemcitabine, 5-fluorouracil, and cisplatin.[115] However, due to their typically high hydrophobicity, high drug resistance, and low tumor specificity, these chemotherapy drugs have low bioavailability, limited therapeutic effects, and serious side effects. Nanomedicine has shown promise in the treatment of breast cancer, both passive targeting based on the EPR effect and active targeting based on overexpressed biomarkers in tumor cells, and can greatly improve the bioavailability of drugs.[116] At present, there is almost a constant stream of research studies reported on composite nanozymes for breast cancer treatment. The following are some key examples of composite nanozymes schemes investigated and reported for breast cancer treatment.

Liu *et al.* developed a cascade catalyzed composite nanozyme with the formula P@Pt@P-Au-FA, in which the Pt nanoparticles in the interlayer and Au nanoparticles on the surface could function as effective catalase mimics and glucose oxidase mimics, respectively, to provide oxygen for PDT, recycle $H_2O_2$, and consume glucose to promote cancer cell starvation treatment.[78] In the hypoxic environment, after 8 min light exposure, the nanoparticles reduced the survival rate of the mouse breast cancer cell 4T1 line to 40% (Fig. 6A), and the detection results for live and dead cells in Fig. 6B also well showed the good inhibition rate of NPs on cancer cells. It can be intuitively found from Fig. 6C and D that in the 4T1 breast cancer mouse model, P@Pt@P-Au-FA NPs combined with laser irradiation significantly inhibited the growth of tumors, in which the inhibition rate even reached 90.88%, while it was also clear that Au NPs could play a vital role in the starvation therapy of cancers.

Lyu *et al.* developed $Fe_3O_4$@$MnO_2$ nanoparticles that integrated MR imaging and treatment capabilities, which could be used in combination with GOx and RT.[104] The core $Fe_3O_4$ of this core–shell-structured nanozyme could trigger the Fenton reaction and generate a large amount of ROS. At the same time, $Fe_3O_4$ has a good magnetic targeting ability and could be used for T2 weighted MRI. The $MnO_2$ in the shell has the ability to consume the GSH in the TME, which can not only consume the generated ROS but may also limit the RT effect. Meanwhile, $Mn^{4+}$ could be used for T1 weighted MRI. Within the test concentration range, the inhibition rate of $Fe_3O_4$@$MnO_2$ combined with GOx and RT on the human breast cancer cell line MCF-7 was 59% and 48.1% higher than that of GOx combined with RT and RT alone, respectively.

**5.2.2 Cervical cancer.** Even though the incidence of cervical cancer in high-income countries has been reduced by more than half in the past 30 years, mostly through better prognosis through effective screening and timely treatment, cervical cancer still ranks seventh globally in incidence and ninth in mortality among all cancers. HeLa cells are immortalized cervical cancer cells that are derived from cancer cell samples taken from a patient in 1951 and that are still thriving today, and are often used in tumor-related research.

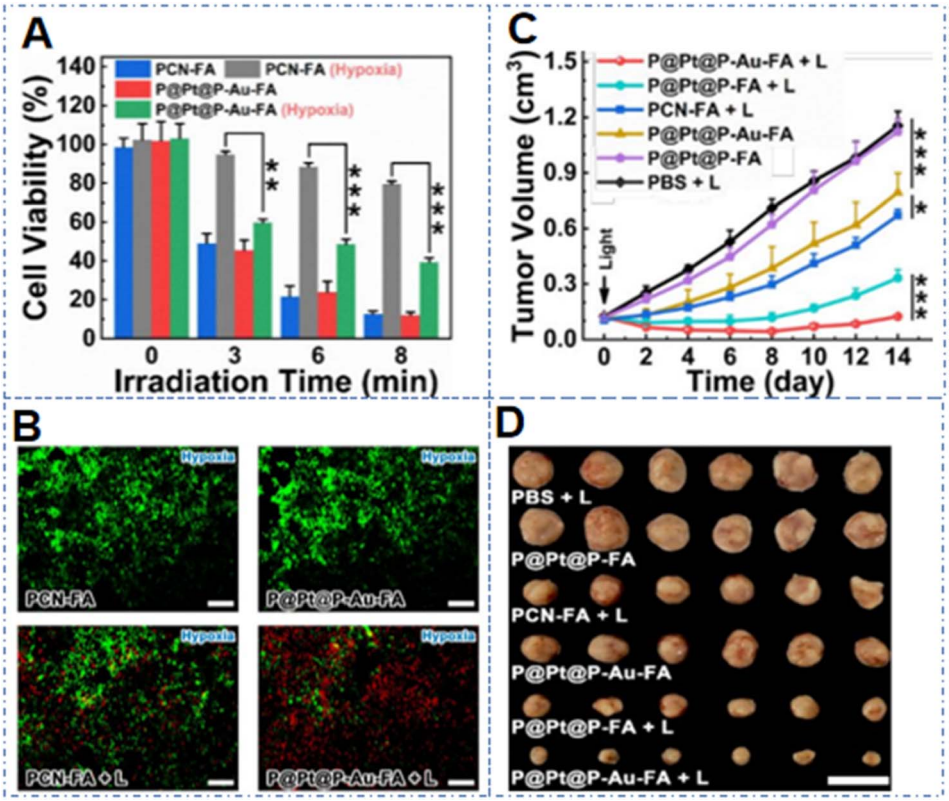


Fig. 6 (A) Viability of 4T1 cells treated with different NPs. (B) Live–dead staining of 4T1 cells treated with different NPs (green indicates viable cells and red indicates dead cells). (C) Tumor growth curves of 4T1 tumor-bearing mice with different treatments; (D) tumors of the model mice after 14 days of treatment. This figure has been adapted/reproduced from ref. 78 with permission from the American Chemical Society, copyright 2019.

Wang *et al.* designed a composite biomimetic nanozyme called HMCGP. They loaded GOD into the cavity of hollow mesoporous copper oxide, and reported the system could achieve the combined treatment of ST, CDT, and PTT through a cascade enzyme method.[82] This nanozyme could catalyze the conversion of endogenous $H_2O_2$ to $O_2$, alleviate the problem of TME hypoxia, which then improved the effectiveness of GOD in catalyzing glucose decomposition. The $Cu^+$ produced by HMC could catalyze the oxidation of endogenous GSH and promote the CDT effect and produce ROS to kill tumors. It was reported that when HMCGP was added to $H_2O_2$, oxygen quickly appeared from the liquid surface and produce more ·OH in a slightly acidic environment at 55 °C. Within the experimental concentration range tested, the HMCGP nanozyme alone showed no significant toxicity to normal mouse fibroblasts. However, after 1064 nm laser irradiation, it was found that the highest concentration of the HMCGP nanozyme could reduce the activity of HeLa cells to 11.6%. Through staining, it was also found that the mitochondria in most cells treated by HMCGP combined with laser irradiation were damaged, with 40.5% of the HeLa cells experiencing apoptosis. In U14 tumor-bearing mouse experiments, the tumor volume of the mice treated with the HMCGP nanozyme combined with laser irradiation was the smallest, and the tumors even disappeared in some mice. The tumor volume was the second smallest in the HMCG nanozyme combined with laser irradiation group, which was thanks to the cascade catalytic effect of the GOD and nanozyme combination.

**5.2.3 Colorectal cancer.** Colorectal cancer is the third most common cancer in the world, with a mortality rate as high as the second highest globally. Yang *et al.* designed a composite nanozyme that combined Pt NPs and carbon NPs for colorectal cancer.[76] Integration of the Pt NPs significantly improved the catalase-like activity of carbon NPs and oxygen production, which promoted oxygen-dependent PDT, while also enhancing the photothermal properties of carbon NPs. In the colon cancer model mice, the anti-tumor rate of the Pt–carbon nanozyme was greater than 90%, significantly higher than that of the carbon nanozyme alone (54%).

The Pt–CuS Janus nanozyme (named PCPT) mentioned in Section 3.2 above not only had the function of catalase to promote the efficacy of SDT and PTT, but could also be used for photoacoustic imaging and near-infrared thermal imaging.[71] It is worth mentioning that under US, the $^1O_2$ production efficiency of the nanozyme was 1.85 times higher than that under 650 nm light irradiation (Fig. 7A). However, in cell experiments, the cell survival rates of the (PCPT + US) group and (PCPT + laser) group, respectively, were decreased to 59.5% and 40.1% (Fig. 7B). The combined treatment by US and laser irradiation could reduce the survival rate of CT26 cells to 19.8%, while in

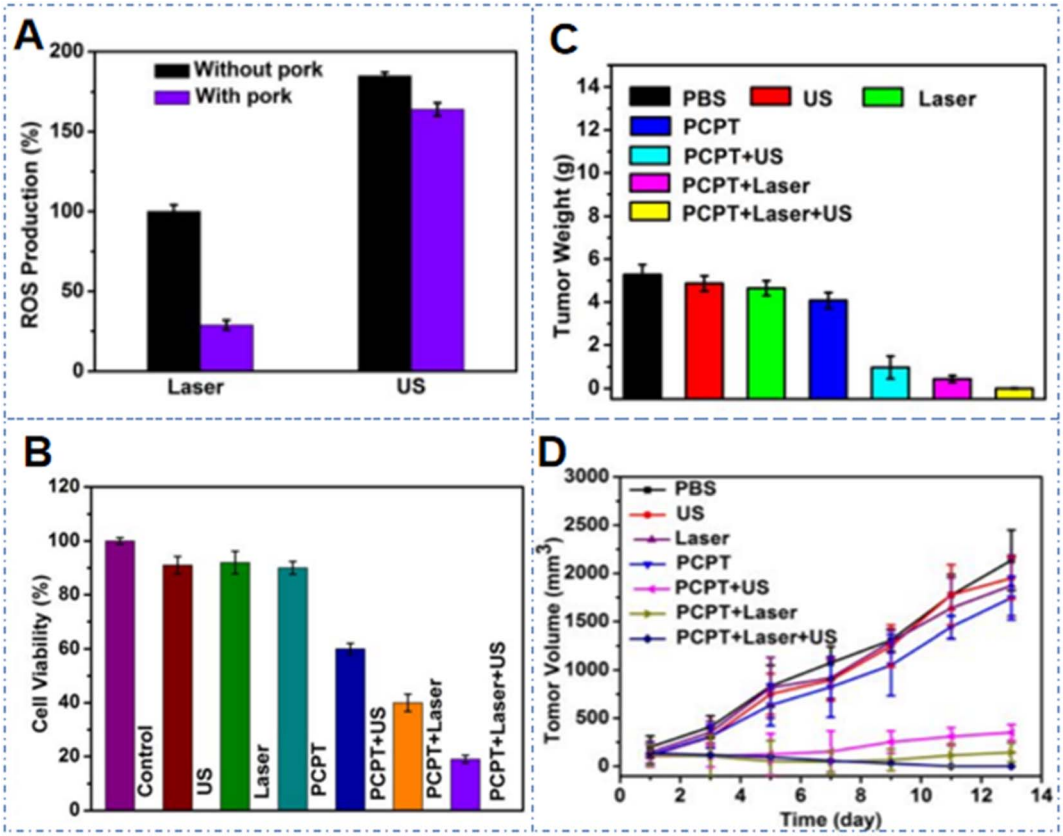


Fig. 7 (A) Relative $^1O_2^-$ production from PCPT after 650 nm NIR light or US irradiation, with or without the screening of pork. (B) Viability of CT26 cells with different treatments. (C) Tumor weight of mice after receiving different treatments. (D) Tumor volume of mice after receiving different treatments. This figure has been adapted/reproduced from ref. 71 with permission from the American Chemical Society, copyright 2019.

the CT26 tumor-bearing mice model, there were particularly significant reductions in the tumor volume and weight in the combined treatment group, indicating that the PCPT nanozyme plays an important role in inhibiting cancer (Fig. 7C and D).

**5.2.4 Liver cancer.** The global incidence rate of liver cancer ranks fifth, but its degree of malignancy is high, and its mortality rate ranks third. It was predicted that from 2020 to 2040, the number of new liver cancer cases and deaths may increase by over 55%.[117] Although traditional HCC treatment strategies, such as surgical resection and TACE, can control the growth of HCC and prolong the survival time of patients, they cannot meet the needs of most patients. Therefore, it is necessary to find a more effective treatment method to improve the quality of life of patients.

Jiang *et al.* designed a CuS@$CeO_2$ nanozyme with a special fusiform shape that could enhance the tumor-penetration ability, combining self-supplied oxygen, a good photothermal conversion ability, and that was RT sensitive and could be used in cancer therapy.[70] When combined with PTT and RT, more than 80% of Hep-G2 cells were killed. After different treatments, the Hep-G2 tumor-bearing mice in the control group experienced rapid tumor growth, while the tumors of the group with CuS@$CeO_2$ NPs-assisted RT/PTT combined treatment did not appear to have grown, and tumor regression was obvious. This design not only allows reducing the RT dose, but more importantly, enables the entire tumor to be treated without recurrence. The Os–Te nanozyme mentioned in Section 3.5 above could combine with PDT/PTT for the treatment of liver cancer.[29] Under hypoxic conditions, it was found that the Os–Te nanozyme greatly improved the therapeutic efficiency of PDT, and the survival rate of RIL-175 cells after treatment was decreased to 10.7%, with a therapeutic efficiency 2.4 times that of Ce6.

**5.2.5 Other cancers.** Melanoma is the most serious skin cancer in the world, accounting for about 1/5th of skin cancers. Melanoma has been a rare disease in history, but the incidence rate of melanoma has been rising in recent years, especially in Europe and North America.[118] ICG/Au/Pt@PDA–PEG NPs, mentioned in Section 3.3 above, were designed by Ciou *et al.* to target melanoma.[77] After NIR laser irradiation (808 nm), the viability of mouse melanoma cells (B16F1 cells) was reduced to 34.5% at the lowest level.

Lung cancer is the malignant cancer with the highest mortality rate, with a mortality rate close to twice that of colorectal cancer, which ranks second. Lung cancer is mainly divided into non-small cell lung cancer and small cell lung cancer, of which 85% of cases are non-small cell lung cancer. The A549 cell line belongs to the typical non-small cell lung cancer. Liu *et al.* prepared a kind of nanozyme that was formed by absorbing various monomers with GOx as the core, including acrylamide, arginine-acrylamide (Arg), ferrocene-acrylate (Fc) and *N*,*N*′-bis(acryloyl)cystamine (BAC). Subsequently, Arg/

 

Fc@GOx nanozymes were formed by an interfacial free radical polymerization.[85] This composite nanozyme utilized the acceleration of enzymes and chemical reactions to induce intracellular RONS (reactive oxygen species and nitrogen) free radical storms, induce cancer cell apoptosis, inhibit tumor growth, and prolong survival rate. During the 17 days observation period, the Arg/Fc@GOx/HA nanozyme showed the most significant tumor inhibition, and in the subsequent 61 days survival experiment, the survival rate of this group of mice was also the highest, reaching 77.8%.

## 6. Conclusions and perspectives

Since their discovery, nanozymes have developed rapidly. Over the past decade, a variety of nanozymes with different catalytic activities have been developed, such as oxidoreductase including POD, CAT, OXD, and SOD, and hydrolases, including phosphatase, nuclease, esterase, and protease. Nanozymes are applied in various fields, such as anti-cancer, anti-bacterial, anti-biofilm, sensing, environmental governance, and antioxidant. In the pursuit of achieving better results, composite nanozymes have been developed, and a large number of studies have reported that composite nanozymes have better catalytic and therapeutic effects than individual nanozymes.

This work summarizes and provides examples of the classification, advantages, and synthesis methods of many nanozymes, as well as their applications in cancer treatment. The anti-tumor principle of composite nanozymes can be summarized as follows: (1) reliance on CAT enzyme activity to consume endogenous $H_2O_2$ or on SOD enzyme activity to produce $O_2$, thereby improving the hypoxia of TME and making other oxygen-dependent therapies feasible; (2) reliance on POD enzyme activity to consume $H_2O_2$ and produce toxic ROS; (3) reliance on GPx enzyme activity to consume endogenous GSH to prevent the consumption of generated ROS; (4) reliance on GOx enzyme activity to consume glucose and generate $H_2O_2$ for recycling, while achieving the effect of starvation therapy; (5) use in combination with other therapies, such as PDT, PTT, CTx, SDT, ST, and RT, where there is a significant synergistic effect that makes combined therapy much better than single therapy.

As mentioned before, composite nanozymes have already played a significant role in various cancers, but there is still a long way to go before the clinical implementation of composite nanozymes can be realized, including:[119–122]

(1) The therapeutic efficacy of nanozymes is contingent upon their *in vivo* stability and activity. Despite the superior catalytic efficiency and stability of composite nanozymes *in vitro*, their performance within the complex tumor microenvironment may be compromised. A profound understanding of the biodistribution and interaction profiles of nanomaterials within biological matrices is essential for the precise quantification of nanozymes' catalytic reactions *in vivo*, thereby facilitating the optimization of nanosystem designs to augment their therapeutic potency.

(2) *In vivo* safety research on nanozymes is inadequate, necessitating a meticulous and systematic dissection of nanozyme pharmacokinetics, encompassing their absorption, distribution, metabolism, and excretion, alongside the dosing regimens necessary for achieving an effective therapeutic impact. It is imperative to scrutinize the toxicity profile of nanozymes under these conditions, including potential hemolytic and coagulation effects, as well as adverse effects on non-target organs and tissues. The strategic incorporation of targeted action in nanozyme design is paramount for enhancing their tumor-specific accumulation. To bridge the gap between preclinical and clinical realms, an expansion of pharmacodynamic and toxicological investigations into larger animal models is imperative, transcending the current reliance on murine studies.

(3) Cancer cells possess a plethora of metabolic pathways, posing a great challenge for rapid metabolic reprogramming. The metabolic regulatory capabilities of extant synthetic nanozymes for oncological applications are relatively circumscribed, predominantly centered on oxidoreductases and often predicated on $H_2O_2$. Given the potential toxicity of $H_2O_2$ in excess, there is an urgent need to diversify the armamentarium of active nanozymes for cancer therapy, with particular emphasis on those independent of $H_2O_2$, such as transferases, isomerases, lyases, and synthases, to broaden the metabolic modulation spectrum of nanozymes in oncological interventions.

(4) The exploration of catalytic kinetics and mechanisms in composite nanozymes is currently lacking. The construction of a holistic theoretical framework for diverse nanozymes, one that amalgamates theoretical computations with empirical validations and harnesses sophisticated characterization methodologies, is imperative for elucidating the molecular underpinnings of nanozyme–cell interactions. This multidimensional approach is pivotal for unraveling the complex functional dynamics of nanozymes within biological systems and for laying the groundwork for the evolution of nanozyme-based therapeutics. By employing omics and single-cell analytical techniques, researchers can probe the molecular intricacies of nanozyme–cell interactions, thereby enhancing the precision and efficacy of nanozyme-mediated therapies. Despite all the challenges that lie ahead, it is strongly believed that through continuous in-depth research, composite nanozymes can be developed that will show excellent performance in clinical applications.

## Data availability

No primary research results, software or code have been included and no new data were generated or analysed as part of this review.

## Conflicts of interest

There are no conflicts to declare.

## Acknowledgements

This work was supported by National Nature Science Foundation of China (grant number: 81271677), and Zhejiang Provincial Natural Science Foundation of China (no. LY21E030011). In

addition, this work was supported by the Medical Science and Technology Project of Zhejiang Province (grant number: 2024KY011, 2025KY561).

## References

1 F. Bray, M. Laversanne, H. Sung, J. Ferlay, R. L. Siegel, I. Soerjomataram and A. Jemal, *Ca-Cancer J. Clin.*, 2024, **74**, 229–263.
2 L. A. Torre, F. Bray, R. L. Siegel, J. Ferlay, J. Lortet-Tieulent and A. Jemal, *Ca-Cancer J. Clin.*, 2015, **65**, 87–108.
3 W. Yin, J. Wang, L. Jiang and Y. James Kang, *Exp. Biol. Med.*, 2021, **246**, 1791–1801.
4 S. Zeng, Q. Tang, M. Xiao, X. Tong, T. Yang, D. Yin, L. Lei and S. Li, *Mater. Today Bio*, 2023, **20**, 100633.
5 X. Li, S. Ai, X. Lu, S. Liu and W. Guan, *RSC Adv.*, 2021, **11**, 35392–35407.
6 P. N. Navya, S. Mehla, A. Begum, H. K. Chaturvedi, R. Ojha, C. Hartinger, M. Plebanski and S. K. Bhargava, *Adv. Healthcare Mater.*, 2023, **12**, 2300768.
7 X. Jiang, J. Wang, X. Deng, F. Xiong, S. Zhang, Z. Gong, X. Li, K. Cao, H. Deng, Y. He, Q. Liao, B. Xiang, M. Zhou, C. Guo, Z. Zeng, G. Li, X. Li and W. Xiong, *J. Exp. Clin. Cancer Res.*, 2020, **39**, 204.
8 Y. Ding, Q. Pan, W. Gao, Y. Pu, K. Luo and B. He, *Biomater. Sci.*, 2023, **11**, 1182–1214.
9 L. Gao, J. Zhuang, L. Nie, J. Zhang, Y. Zhang, N. Gu, T. Wang, J. Feng, D. Yang, S. Perrett and X. Yan, *Nat. Nanotechnol.*, 2007, **2**, 577–583.
10 S. Ahmadi, K. Rahimizadeh, A. Shafiee, N. Rabiee and S. Iravani, *Process Biochem.*, 2023, **131**, 154–174.
11 A. Deshwal, K. Saxena, G. Sharma, Rajesh, F. A. Sheikh, C. S. Seth and R. M. Tripathi, *Int. J. Biol. Macromol.*, 2024, **256**, 128272.
12 S. Thangudu and C.-H. Su, *Biomolecules*, 2021, **11**, 1015.
13 D. Xu, L. Wu, H. Yao and L. Zhao, *Small*, 2022, **18**, 2203400.
14 Y. Huang, J. Ren and X. Qu, *Chem. Rev.*, 2019, **119**, 4357–4412.
15 X. Zhang, X. Chen and Y. Zhao, *Nano-Micro Lett.*, 2022, **14**, 95.
16 C. Lu, X. Liu, Y. Li, F. Yu, L. Tang, Y. Hu and Y. Ying, *ACS Appl. Mater. Interfaces*, 2015, **7**, 15395–15402.
17 W. B. Direrssa, G. Getachew, C. H. Hsiao, A. Wibrianto, A. S. Rasal, C. C. Huang and J. Y. Chang, *Mater. Today Chem.*, 2022, **26**, 101158.
18 X. Wang and L. Cheng, *Coord. Chem. Rev.*, 2020, **419**, 213393.
19 B. Xu, Z. Huang, Y. Liu, S. Li and H. Liu, *Nano Today*, 2023, **48**, 101690.
20 H. Li, M. Wei, X. Lv, Y. Hu, J. Shao, X. Song, D. Yang, W. Wang, B. Li and X. Dong, *J. Innovative Opt. Health Sci.*, 2022, **15**, 2230009.
21 D. Yin, H. Yang, S. Wang, Z. Yang, Q. Liu, X. Zhang and X. Zhang, *Colloids Surf., A*, 2020, **607**, 125466.
22 S. Wang, J. Zhao, L. Zhang, C. Zhang, Z. Qiu, S. Zhao, Y. Huang and H. Liang, *Adv. Healthcare Mater.*, 2022, **11**, e2102073.
23 H. Xu, Z. Zhang, L. Zhang, Z. Chen and S. Wang, *J. Colloid Interface Sci.*, 2022, **625**, 544–554.
24 F. Cheng, S. Wang, H. Zheng, S. Yang, L. Zhou, K. Liu, Q. Zhang and H. Zhang, *Colloids Surf., B*, 2021, **205**, 111878.
25 M. Wang, M. Chang, Q. Chen, D. Wang, C. Li, Z. Hou, J. Lin, D. Jin and B. Xing, *Biomaterials*, 2020, **252**, 120093.
26 C. Cao, H. Zou, N. Yang, H. Li, Y. Cai, X. Song, J. Shao, P. Chen, X. Mou, W. Wang and X. Dong, *Adv. Mater.*, 2021, **33**, 2106996.
27 C. Wang, Y. Li, W. Yang, L. Zhou and S. Wei, *Adv. Healthcare Mater.*, 2021, **10**, e2100601.
28 H. Wu, Q. Jiang, K. Luo, C. Zhu, M. Xie, S. Wang, Z. Fei and J. Zhao, *J. Nanobiotechnol.*, 2021, **19**, 203.
29 S. Kang, Y. G. Gil, G. Yim, D. H. Min and H. Jang, *ACS Appl. Mater. Interfaces*, 2021, **13**, 44124–44135.
30 J. Yang, L. Fang, R. Jiang, L. Qi, Y. Xiao, W. Wang, I. Ismail and X. Fang, *Adv. Healthcare Mater.*, 2023, e2300490, DOI: **10.1002/adhm.202300490**.
31 B. Jiang, D. Duan, L. Gao, M. Zhou, K. Fan, Y. Tang, J. Xi, Y. Bi, Z. Tong, G. F. Gao, N. Xie, A. Tang, G. Nie, M. Liang and X. Yan, *Nat. Protoc.*, 2018, **13**, 1506–1520.
32 X. Hong, X. Xu, Z. Liu, S. Liu, J. Yu, M. Wu, Y. Ma and Q. Shuai, *Nanotechnology*, 2021, **32**, 465701.
33 Y. Yan, Y. Hou, H. Zhang, W. Gao, R. Han, J. Yu, L. Xu and K. Tang, *Colloids Surf., B*, 2021, **208**, 112103.
34 N. Singh, M. A. Savanur, S. Srivastava, P. D'Silva and G. Mugesh, *Angew Chem. Int. Ed. Engl.*, 2017, **56**, 14267–14271.
35 J. Mu, Y. Wang, M. Zhao and L. Zhang, *Chem. Commun.*, 2012, **48**, 2540–2542.
36 Z. Zhu, Z. Guan, S. Jia, Z. Lei, S. Lin, H. Zhang, Y. Ma, Z. Q. Tian and C. J. Yang, *Angew Chem. Int. Ed. Engl.*, 2014, **53**, 12503–12507.
37 W. He, Y.-T. Zhou, W. G. Wamer, M. D. Boudreau and J.-J. Yin, *Biomaterials*, 2012, **33**, 7547–7555.
38 Y. Li, K.-H. Yun, H. Lee, S.-H. Goh, Y.-G. Suh and Y. Choi, *Biomaterials*, 2019, **197**, 12–19.
39 J. L. Qingqing Wang, L. He, S. Liu and P. Yang, *Nanoscale*, 2023, **15**, 12455–12463.
40 A. Asati, S. Santra, C. Kaittanis, S. Nath and J. M. Perez, *Angew. Chem., Int. Ed.*, 2009, **48**, 2308–2312.
41 I. Celardo, J. Z. Pedersen, E. Traversa and L. Ghibelli, *Nanoscale*, 2011, **3**, 1411.
42 J. Mu, X. Zhao, J. Li, E.-C. Yang and X.-J. Zhao, *J. Mater. Chem. B*, 2016, **4**, 5217–5221.
43 X. Yu, Y. Wang, J. Zhang, J. Liu, A. Wang and L. Ding, *Adv. Healthcare Mater.*, 2023, **13**, 2302023.
44 C. Hao, A. Qu, L. Xu, M. Sun, H. Zhang, C. Xu and H. Kuang, *J. Am. Chem. Soc.*, 2018, **141**, 1091–1099.
45 P. Ling, Q. Zhang, T. Cao and F. Gao, *Angew. Chem., Int. Ed.*, 2018, **57**, 6819–6824.
46 P. K. Boruah and M. R. Das, *J. Hazard. Mater.*, 2020, **385**, 121516.
47 S. Maddheshiya and S. Nara, *Front. Bioeng. Biotechnol.*, 2022, **10**, 880214.
48 L. Li, Z. Lin, X. Xu, W. Wang, H. Chen, Z. Feng, Z. Yang and J. Hao, *ACS Appl. Mater. Interfaces*, 2023, **15**, 41224–41236.

49 M. Wang, J. Li, J. Liu, Y. Huang, L. Yang, C. Zhu, Y. Zhang, X. Gui, H. Peng and M. Chu, *J. Colloid Interface Sci.*, 2024, **676**, 110–126.
50 J. Ma, Q. Yao, S. Lv, J. Yi, D. Zhu, C. Zhu, L. Wang and S. Su, *J. Nanobiotechnol.*, 2024, **22**, 596.
51 S. Cui, B. Wang, C. Zhai, S. Wei, H. Zhang and G. Sun, *J. Mater. Chem. B*, 2023, **11**, 7986–7997.
52 J. Liu, B. Yu, M. Rong, W. Sun and L. Lu, *Nano Today*, 2024, **54**, 102113.
53 B. Li, H. Shen, Q. Liu, X. Liu, J. Cai, L. Zhang, D. Wu, Y. Xie, G. Xie and W. Feng, *Sens. Actuators, B*, 2023, **386**, 133762.
54 X. Zhang, Y. Liu, J. Doungchawee, L. J. Castellanos-García, K. N. Sikora, T. Jeon, R. Goswami, S. Fedeli, A. Gupta, R. Huang, C.-M. Hirschbiegel, R. Cao-Milán, P. K. D. Majhi, Y. A. Cicek, L. Liu, D. J. Jerry, R. W. Vachet and V. M. Rotello, *J. Controlled Release*, 2023, **357**, 31–39.
55 S. Zhang, Y. Liu, S. Sun, J. Wang, Q. Li, R. Yan, Y. Gao, H. Liu, S. Liu, W. Hao, H. Dai, C. Liu, Y. Sun, W. Long, X. Mu and X.-D. Zhang, *Theranostics*, 2021, **11**, 2806–2821.
56 Q. Wang, C. Cheng, S. Zhao, Q. Liu, Y. Zhang, W. Liu, X. Zhao, H. Zhang, J. Pu, S. Zhang, H. Zhang, Y. Du and H. Wei, *Angew. Chem., Int. Ed.*, 2022, **61**, e202201101.
57 X. Zhang, X. Li, M. Fu, J. O. A. Machuki, W. Wang, L. Wu, Q. Zhao, N. Xin, L. Hua and F. Gao, *Chem. Eng. J.*, 2024, **481**, 148745.
58 H. Liu, Z. Deng, Z. Zhang, W. Lin, M. Zhang and H. Wang, *Matter*, 2024, **7**, 977–990.
59 B. Yang, L. Cao, K. Ge, C. Lv, Z. Zhao, T. Zheng, S. Gao, J. Zhang, T. Wang, J. Jiang and Y. Qin, *Small*, 2024, **20**, 2401110.
60 W. Shen, G. Han, L. Yu, S. Yang, X. Li, W. Zhang and P. Pei, *Int. J. Nanomed.*, 2022, **17**, 1397–1408.
61 L. He, Q. Ji, B. Chi, S. You, S. Lu, T. Yang, Z. Xu, Y. Wang, L. Li and J. Wang, *Colloids Surf., B*, 2023, **222**, 113058.
62 K. Nie, L. Zhu, Y. Chen, L. Yu, M. Chang, Y. Chen and H. Yu, *Nano Today*, 2023, **53**, 102050.
63 K. Xu, X. Wu, Y. Cheng, J. Yan, Y. Feng, R. Chen, R. Zheng, X. Li, P. Song, Y. Wang and H. Zhang, *Nanoscale*, 2020, **12**, 23159–23165.
64 X. Zhong, X. Wang, L. Cheng, Y. A. Tang, G. Zhan, F. Gong, R. Zhang, J. Hu, Z. Liu and X. Yang, *Adv. Funct. Mater.*, 2019, **30**, 1907954.
65 C. Gong, J. Zhao, X. Meng, Z. Yang and H. Dong, *Chem. Eng. J.*, 2022, **435**, 135083.
66 F. Gong, L. Cheng, N. Yang, O. Betzer, L. Feng, Q. Zhou, Y. Li, R. Chen, R. Popovtzer and Z. Liu, *Adv. Mater.*, 2019, **31**, e1900730.
67 S. Li, L. Shang, B. Xu, S. Wang, K. Gu, Q. Wu, Y. Sun, Q. Zhang, H. Yang, F. Zhang, L. Gu, T. Zhang and H. Liu, *Angew Chem. Int. Ed. Engl.*, 2019, **58**, 12624–12631.
68 D. Jana, B. He, Y. Chen, J. Liu and Y. Zhao, *Adv. Mater.*, 2024, **36**, 2206401.
69 S. Yu, D. Jang, S. K. Maji, K. Chung, J. S. Lee, F. Marques Mota, J. Wang, S. Kim and D. H. Kim, *J. Ind. Eng. Chem.*, 2021, **104**, 106–116.
70 W. Jiang, X. Han, T. Zhang, D. Xie, H. Zhang and Y. Hu, *Adv. Healthcare Mater.*, 2020, **9**, e1901303.
71 S. Liang, X. Deng, Y. Chang, C. Sun, S. Shao, Z. Xie, X. Xiao, P. Ma, H. Zhang, Z. Cheng and J. Lin, *Nano Lett.*, 2019, **19**, 4134–4145.
72 S. Liang, X. Deng, G. Xu, X. Xiao, M. Wang, X. Guo, P. A. Ma, Z. Cheng, D. Zhang and J. Lin, *Adv. Funct. Mater.*, 2020, **30**, 1908598.
73 S. Y. Yin, G. Song, Y. Yang, Y. Zhao, P. Wang, L. M. Zhu, X. Yin and X. B. Zhang, *Adv. Funct. Mater.*, 2019, **29**, 1901417.
74 Z. Wang, Y. Zhang, E. Ju, Z. Liu, F. Cao, Z. Chen, J. Ren and X. Qu, *Nat. Commun.*, 2018, **9**, 3334.
75 M. Chen, J. Song, J. Zhu, G. Hong, J. An, E. Feng, X. Peng and F. Song, *Adv. Healthcare Mater.*, 2021, **10**, 2101049.
76 Y. Yang, D. Zhu, Y. Liu, B. Jiang, W. Jiang, X. Yan and K. Fan, *Nanoscale*, 2020, **12**, 13548–13557.
77 T. Y. Ciou, C. Korupalli, T. H. Chou, C. H. Hsiao, G. Getachew, S. Bela and J. Y. Chang, *ACS Appl. Bio Mater.*, 2021, **4**, 5650–5660.
78 C. Liu, J. Xing, O. U. Akakuru, L. Luo, S. Sun, R. Zou, Z. Yu, Q. Fang and A. Wu, *Nano Lett.*, 2019, **19**, 5674–5682.
79 P. Dong, W. Wang, M. Pan, W. Yu, Y. Liu, T. Shi, J. Hu, Y. Zhou, S. Yu, F. Wang and X. Liu, *ACS Appl. Mater. Interfaces*, 2021, **13**, 16075–16083.
80 D. Zhang, Z. Ye, L. Wei, H. Luo and L. Xiao, *ACS Appl. Mater. Interfaces*, 2019, **11**, 39594–39602.
81 Y. Zhu, Z. Wang, R. Zhao, Y. Zhou, L. Feng, S. Gai and P. Yang, *ACS Nano*, 2022, **16**, 3105–3118.
82 J. Wang, J. Ye, W. Lv, S. Liu, Z. Zhang, J. Xu, M. Xu, C. Zhao, P. Yang and Y. Fu, *ACS Appl. Mater. Interfaces*, 2022, **14**, 40645–40658.
83 Z. Xu, P. Sun, J. Zhang, X. Lu, L. Fan, J. Xi, J. Han and R. Guo, *Chem. Eng. J.*, 2020, **399**, 125797.
84 H. Yang, B. Xu, S. Li, Q. Wu, M. Lu, A. Han and H. Liu, *Small*, 2021, **17**, e2007090.
85 X. Liu, W. Li, M. Wang, N. Liu, Q. Yang, Y. He, D. Hu, R. Zhu and L. Yin, *Small Methods*, 2023, **7**, e2201641.
86 F. Wu, Y. Du, J. Yang, B. Shao, Z. Mi, Y. Yao, Y. Cui, F. He, Y. Zhang and P. Yang, *ACS Nano*, 2022, **16**, 3647–3663.
87 Q. Fu, C. Wei and M. Wang, *ACS Nano*, 2024, **18**, 12049–12095.
88 X. Zhou, S. Feng, Q. Xu, Y. Li, J. Lan, Z. Wang, Y. Ding, S. Wang and Q. Zhao, *Acta Biomater.*, 2025, **191**, 1–28.
89 N. Feng, Y. Liu, X. Dai, Y. Wang, Q. Guo and Q. Li, *RSC Adv.*, 2022, **12**, 1486–1493.
90 M. Tang, Z. Zhang, C. Ding, J. Li, Y. Shi, T. Sun and C. Chen, *J. Colloid Interface Sci.*, 2022, **627**, 299–307.
91 Y. Qian, J. Zou, J. Zhang, X. Wang, X. Meng, Y. Lin, W. Lin, M. Zhang and H. Wang, *Chem. Eng. J.*, 2024, **490**, 151867.
92 M. Luo, F.-K. Zhao, Y.-M. Wang and J. Bian, *J. Transl. Med.*, 2024, **22**, 814.
93 P. T. Nguyen, J. Lee, A. Cho, M. S. Kim, D. Choi, J. W. Han, M. I. Kim and J. Lee, *Adv. Funct. Mater.*, 2022, **32**, 2112428.
94 X. Zeng, H. Wang, Y. Ma, X. Xu, X. Lu, Y. Hu, J. Xie, X. Wang, Y. Wang, X. Guo, L. Zhao and J. Li, *ACS Appl. Mater. Interfaces*, 2023, **15**, 13941–13955.

95 S.-B. He, L. Yang, Y. Yang, H. A. A. Noreldeen, G.-W. Wu, H.-P. Peng, H.-H. Deng and W. Chen, *Carbohydr. Polym.*, 2022, **298**, 120120.
96 J. Zhou, X.-J. Yang, Q. Yu, X.-L. Li, H.-Y. Chen and J.-J. Xu, *ACS Appl. Nano Mater.*, 2022, **5**, 7009–7018.
97 S. Li, X. Zhao, H. Ding, J. Chang, X. Qin, F. He, X. Gao, S. Gai and P. Yang, *Chem. Eng. J.*, 2023, **473**, 145414.
98 S. Feng, J. Wang, X. Mu, G. Gu, Y. Wang, J. Lu, S. Wang and Q. Zhao, *Colloids Surf., B*, 2023, **222**, 113095.
99 N. Saravanan, P. Ganesh, S. Pitchaimuthu and A. Sundaramurthy, *Surf. Interfaces*, 2023, **41**, 103225.
100 C. Dong, X. Dai, X. Wang, Q. Lu, L. Chen, X. Song, L. Ding, H. Huang, W. Feng, Y. Chen and M. Chang, *Adv. Mater.*, 2022, **34**, 2205680.
101 Z. Chen, J.-J. Yin, Y.-T. Zhou, Y. Zhang, L. Song, M. Song, S. Hu and N. Gu, *ACS Nano*, 2012, **6**, 4001–4012.
102 S. Dong, Y. Dong, B. Liu, J. Liu, S. Liu, Z. Zhao, W. Li, B. Tian, R. Zhao, F. He, S. Gai, Y. Xie, P. Yang and Y. Zhao, *Adv. Mater.*, 2022, **34**, 2107054.
103 S. Dong, Y. Dong, T. Jia, S. Liu, J. Liu, D. Yang, F. He, S. Gai, P. Yang and J. Lin, *Adv. Mater.*, 2020, **32**, e2002439.
104 M. Lyu, D. Zhu, X. Kong, Y. Yang, S. Ding, Y. Zhou, H. Quan, Y. Duo and Z. Bao, *Adv. Healthcare Mater.*, 2020, **9**, e1901819.
105 Z. Hu, X. Zhou, W. Zhang, L. Zhang, L. Li, Y. Gao and C. Wang, *J. Colloid Interface Sci.*, 2025, **679**, 375–383.
106 X. Han, Y. Li, Y. Zhou, Z. Song, Y. Deng, J. Qin and Z. Jiang, *Mater. Des.*, 2021, **204**, 109646.
107 X. Meng, H. Fan, L. Chen, J. He, C. Hong, J. Xie, Y. Hou, K. Wang, X. Gao, L. Gao, X. Yan and K. Fan, *Nat. Commun.*, 2024, **15**, 1626.
108 X. Meng and J. Gao, *Arabian J. Chem.*, 2024, **17**, 105626.
109 S. Liang, X. Deng, G. Xu, X. Xiao, M. Wang, X. Guo, P. a. Ma, Z. Cheng, D. Zhang and J. Lin, *Adv. Funct. Mater.*, 2020, **30**, 1908598.
110 Z. Zhou, J. Huang, Z. Zhang, L. Zhang, Y. Cao, Z. Xu, Y. Kang and P. Xue, *Chem. Eng. J.*, 2022, **435**, 135085.
111 Y. Yin, L. Zhu, T. Jiang, R. Chai, Y. Zhang, T. Li, K. Wang, S. Wang and Q. Zhang, *Chem. Eng. J.*, 2024, **501**, 157762.
112 J. Xing, X. Ma, Y. Yu, Y. Xiao, L. Chen, W. Yuan, Y. Wang, K. Liu, Z. Guo, H. Tang, K. Fan and W. Jiang, *Adv. Sci.*, 2024, **2024**, 2405597.
113 M. Arnold, E. Morgan, H. Rumgay, A. Mafra, D. Singh, M. Laversanne, J. Vignat, J. R. Gralow, F. Cardoso, S. Siesling and I. Soerjomataram, *Breast*, 2022, **66**, 15–23.
114 M. Akram, M. Iqbal, M. Daniyal and A. U. Khan, *Biol. Res.*, 2017, **50**, 33.
115 R. Fan, X. Tao, X. Zhai, Y. Zhu, Y. Li, Y. Chen, D. Dong, S. Yang and L. Lv, *Biomed. Pharmacother.*, 2023, **161**, 114444.
116 A. A. Ashkarran, Z. Lin, J. Rana, H. Bumpers, L. Sempere and M. Mahmoudi, *Small*, 2023, **20**, 2301385.
117 H. Rumgay, M. Arnold, J. Ferlay, O. Lesi, C. J. Cabasag, J. Vignat, M. Laversanne, K. A. McGlynn and I. Soerjomataram, *J. Hepatol.*, 2022, **77**, 1598–1606.
118 M. Arnold, D. Singh, M. Laversanne, J. Vignat, S. Vaccarella, F. Meheus, A. E. Cust, E. de Vries, D. C. Whiteman and F. Bray, *JAMA Dermatol.*, 2022, **158**, 495–503.
119 X. Xu, Y. Zhang, C. Meng, W. Zheng, L. Wang, C. Zhao and F. Luo, *J. Mater. Chem. B*, 2024, **12**, 9111–9143.
120 Q. Zhang, L. Song and K. Zhang, *Mater. Chem. Front.*, 2023, **7**, 44–64.
121 N. Tagaras, H. Song, S. Sahar, W. Tong, Z. Mao and T. Buerki-Thurnherr, *Adv. Sci.*, 2024, **11**, 2407816.
122 X. Li, J. Hu, Q. Zhao, W. Yao, Z. Jing and Z. Jin, *J. Transl. Med.*, 2024, **22**, 1033.